

HUGHES AIRCRAFT COMPANY
ELECTRON DYNAMICS DIVISION
3100 W. LOMITA BOULEVARD
TORRANCE, CALIFORNIA

HAC/EDD No. W-2241
NASA No. 66525

SEPTEMBER 1967

FINAL REPORT

20 WATT X-BAND TWT DEVELOPMENT
NASA CONTRACT NO. NAS 1-5905

Distribution of this report is provided in the interest
of information exchange. Responsibility for the contents
resides in the author or organization that prepared it.

TABLE OF CONTENTS

| <u>Section</u> | <u>Page No.</u> |
|--|-----------------|
| Abstract | iii |
| Introduction | 1 |
| Traveling-wave Tube | 2 |
| Summary | 2 |
| Initial Development Phase | 2 |
| Second Phase | 7 |
| Third Phase | 18 |
| Power Supply | 38 |
| Introduction | 38 |
| Circuit Description | 38 |
| Voltage Regulator | 38 |
| Conclusions and Recommendations | 46 |
| Environmental and Life Improvement | 46 |
| Efficiency Improvement | 47 |
| Cost Improvement | 47 |
| Weight and Size Improvement | 47 |
| Appendix A - 219H TWT Electrical Operating Parameters | 48 |
| Appendix B - 219H TWT Mechanical Properties | 49 |
| Appendix C - 1153H Electrical and Mechanical Description | 50 |
| Appendix D - Definitions | 51 |

LIST OF ILLUSTRATIONS

| <u>Figure No.</u> | | <u>Page No.</u> |
|-------------------|--|-----------------|
| 1A | 219H TWT | 3 |
| 1B | Model 219H TWT vacuum assembly and package configuration. | 3 |
| 2 | Power, efficiency and gain vs frequency for model 219H TWT, Serial Number 1. | 8 |
| 3 | Basic efficiency vs output section small signal gain. | 11 |
| 4. | Power, gain and efficiency vs beam voltage for model 219H TWT, Serial Number 16. | 12 |
| 5. | Basic efficiency vs γr_b parameter for model 219H TWT Serial Numbers as noted. | 14 |
| 6. | Helix and anode interception vs collector depression for model 219H TWT, Serial Number 16. | 15 |
| 7. | Beam transmission vs collector depression with electronic efficiency improvement factor as a parameter. | 16 |
| 8. | Collector depression efficiency improvement vs relative beam diameter for model 219H TWT, Serial Number noted. | 17 |
| 9. | Efficiency parameters vs beam diameter for model 219H TWT, Serial Numbers noted. | 19 |
| 10. | Power, gain and efficiency vs frequency for model 219H TWT, Serial Number 16. | 20 |
| 11. | Efficiency parameter vs beam diameter for model 219H TWT, Serial Number 17 relative to phase 2 results. | 21 |
| 12. | Power, gain and efficiency vs frequency for model 219H TWT, Serial Number 17. | 23 |
| 13A. | Power output vs power input. | 26 |
| 13B. | Power output vs power input. | 27 |
| 13C. | Power output vs power input. | 28 |
| 13D. | Power output vs power input. | 29 |
| 14A. | Saturated power variation vs frequency. | 30 |
| 14B. | Saturated power variation vs frequency. | 31 |
| 15. | Hot output and hot input match vs frequency. | 33 |

| | | |
|-----|--|----|
| 16. | Power, gain and efficiency vs beam voltage for model 219H TWT, Serial Number 17. | 34 |
| 17. | Power, gain and efficiency vs beam voltage for model 219H TWT, Serial Number 17. | 35 |
| 18. | Phase shift vs helix voltage for model 219H TWT Serial Number 1. | 36 |
| 19. | Block diagram. | 39 |
| 20. | Schematic diagram - EMPS 241. | 41 |
| 21. | Outline and mounting TWTA 1153H. | 45 |

ABSTRACT

The results of a program to develop a 20 watt, 8.4 to 8.5 GHz traveling-wave tube amplifier suitable for spacecraft applications are summarized. The basic traveling-wave tube development consisted primarily of extending the state of the art to obtain a required 35% efficiency at X-band. A number of tubes were built using various helix and gun designs to achieve the required results. Helix changes were made in order to properly center the tube within the desired operating frequency range. Different gun perveances were tried in order to optimize tube efficiency obtainable by means of depressed collector operation. In all, a total of seventeen tubes were constructed, with the last tube, Serial Number 17, providing the specified power, gain and efficiency performance.

The accompanying power supply is a space type, high efficiency traveling-wave tube power supply which was purchased from Engineered Magnetics, a Division of Gulton Industries.

INTRODUCTION

This report presents a technical discussion of work accomplished under NASA contract No. NAS 1-5905. The program was initiated to develop and deliver one (1) traveling-wave tube amplifier suitable for space craft applications. The amplifier was to provide a nominal 20 watts of RF power at a center frequency around 8.4 to 8.5 GHz. The specifications were typical of those required for space craft applications at lower frequencies, however, no such device existed at X-band nor was there any existing traveling-wave tube similar enough to that required to allow simple scaling. Further, there was considerable doubt concerning the feasibility of obtaining 35% traveling-wave tube efficiency at X-band since the best existing tubes were only about 27 to 28% efficient. The high value of efficiency was being achieved on the most advanced tubes at S-band and C-band but scaling these tubes would yield theoretically only about 30% efficiency. Obtaining 35% efficiency at X-band is similar to obtaining about 40% at C-band.

Hughes approached the program primarily as a tube development which required an extension of the state of the art with respect to efficiency and the major effort was devoted to the end. The tube discussion, given in the following section, forms the largest portion of the report. The power supply was purchased as an off the shelf unit and is given only cursory attention in the subsequent section.

The engineer primarily responsible for the tube development was P. S. Wolcott. Other making major contributions to the program were B. L. Phillips and E. Urban. Bruce Gladstone of Engineered Magnetics, a division of Gulton Industries, was responsible for the Power Supply.

TRAVELING-WAVE TUBE

I. SUMMARY

The Model 219H traveling-wave tube development is described herein. Seventeen (17) tubes have been constructed. The last tube, Serial Number 17, provides the specified power, gain, and efficiency performance. A photograph of Model 219H traveling-wave tubes in various stages of package assembly is shown in figures 1a and 1b.

For purposes of discussion, the progress of traveling-wave tube development may be divided into three phases. The first phase encompasses the general evaluation and selection of the major parameters, perveance, and beam voltage, the design of the vacuum envelope, and the determination of the gun, helix and collector configurations. The second phase consists of several iterative perturbations on the resultant first phase design aimed at establishing optimum performance; primarily optimum overall efficiency. The third phase includes the introduction of additional techniques to improve on the second phase results, and the resulting improved performance.

General electrical and mechanical properties as well as definitions are listed as appendices.

II. INITIAL DEVELOPMENT PHASE

Seven tubes were built and tested in this phase. Two gun designs were accomplished. The significant developments are as follows:

A. Perveance Selection

Two traveling-wave tube designs based on perveance values of 0.20 and 0.375 microperves were investigated. The 0.20 microperveance design is superior because it permits enhanced col-

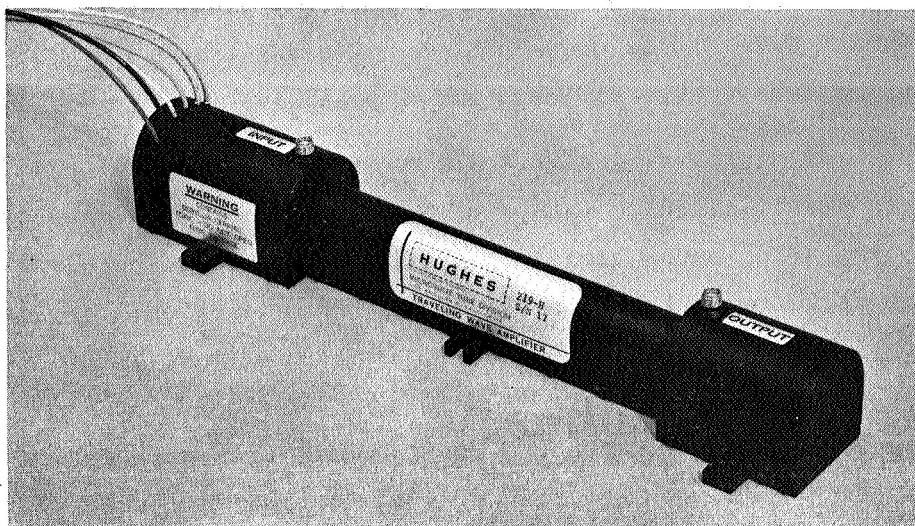


Figure 1A 219H TWT.

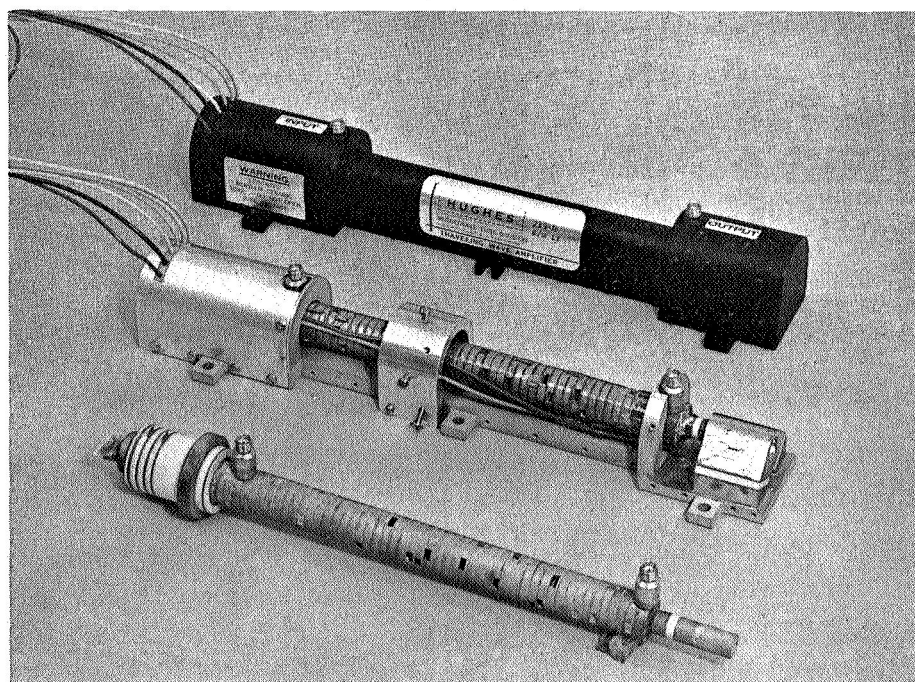


Figure 1B Model 219H TWT vacuum assembly and package configuration.

lector depression and beam transmission thus leading to higher overall efficiency. Table 1 shows a comparison of the two designs. Three tubes were constructed using the 0.375 microperv design before this approach was dropped.

The 0.20 microperv design has proved to be quite adequate with beam transmission in excess of 94.5% for collector depression voltages in excess of 54% of the beam voltage. These parameters are discussed further in the second phase section.

B. Gun Development

Two 0.20 micropervance gun designs have been developed to existing hardware. They are designed to provide conservative loading at different beam minimum (slow wave circuit entrance condition) diameters. Significant characteristics of these guns are indicated in Table 2. Here it may be seen that the 156 C and the 161 B have comparable conservative cathode loading while the 161 B provides the smaller entrance beam (minimum) diameter. The 156 D has a beam size similar to the 161 B but a less conservative cathode loading as a result of down scaling from the conservatively loaded 156 C. The 156 D provided a development substitute for the 161 B while parts of the latter were being fabricated.

The optimum tube performance has been achieved using the 156 C gun.

Both gun designs were accomplished by the Electron Optics Group of this Division.

C. TWT Circuit Development

Four tubes comprising three circuit design iterations of the 0.20 microperv approach were built and tested in this phase. All four used an interim 142-2B gun. While the initial design (Serial Numbers 1 and 3) demonstrated respectable power,

MODEL 219H TWT DEVELOPMENT

| PERVEANCE | RF OUTPUT POWER | SAT GAIN | BASIC EFFI- CIENCY | CIRCUIT LENGTH | BEAM TRANS- MISSION | COLLECTOR DEPRESSION | EFFICIENCY IMPROVE- MENT | MAGNET FOCUSING FIELD |
|------------------------|--------------------|-------------|--------------------------|-------------------|---------------------------|-------------------------|--------------------------------|-----------------------------|
| 0.200×10^{-6} | >20W | >30dB | >14% | 6.3 in | >94% | >56% | >2.1 | 1400-1600 GAUSS |
| 0.375×10^{-6} | >20W | >30dB | >16% | 4.32 in | 90% | 50% | 1.8 | 1800-1900 GAUSS |

FREQUENCY = 8.0-8.5 KMc

Table 1 Comparison of perveance designs.

$$\text{PERVEANCE} = 0.20 \times 10^{-6}$$

| GUN TYPE | CATHODE DIA. | CATHODE LOADING | BEAM MIN. DIA. | AREA COMP. RATIO |
|----------|--------------|------------------------|----------------|------------------|
| I56 C | .200 In | 196 mA/cm ² | .040 In | 25 |
| I56 D | .172 In | 264 mA/cm ² | .034 In | 25 |
| I6I B | .208 In | 181 mA/cm ² | .034 In | 36 |

Table 2 Relevant electron gun designs for the 219H TWT.

efficiency, beam transmission and collector depression characteristics, the frequency was centered too low. This is demonstrated in Figure 2. Two design iterations (Serial Numbers 6 and 7) were made before proper frequency centering was accomplished. Serial Number 6 incorporated a pitch change. Serial Number 7 utilized a full helix geometry scaling. Both raised the frequency about half the required amount. Serial Number 7 showed an improvement in efficiency while Serial Number 6 showed a decrease. It was concluded that a further pitch increase would require a perveance reduction and would result in a longer tube for equivalent gain and optimum efficiency. Since the Serial Number 7 results were promising, the final frequency centering was accomplished by further helix geometry scaling, maintaining the previous beam voltage and perveance.

III. SECOND PHASE

Test results on Serial Numbers 8 and 9 demonstrated proper frequency centering. At this point, the helix and collector dimensions were established. Serial Numbers 8 through 16 incorporated variations in beam geometry (by gun selection and focusing magnetic field selection), variation in output section length and small changes in the attenuator configuration. Table 3 summarizes these design perturbations.

It has been previously established that optimum depressed electronic efficiency for any given slow wave circuit configuration over a limited range of beam interaction conditions, depends on several factors; sufficient output section gain, optimum overvoltage condition, optimum beam diameter (γr_b), and optimum collector depression-beam transmission efficiency improvement factor. The effect of these several factors on efficiency has been experimentally determined and an optimum compromise beam geometry selected.

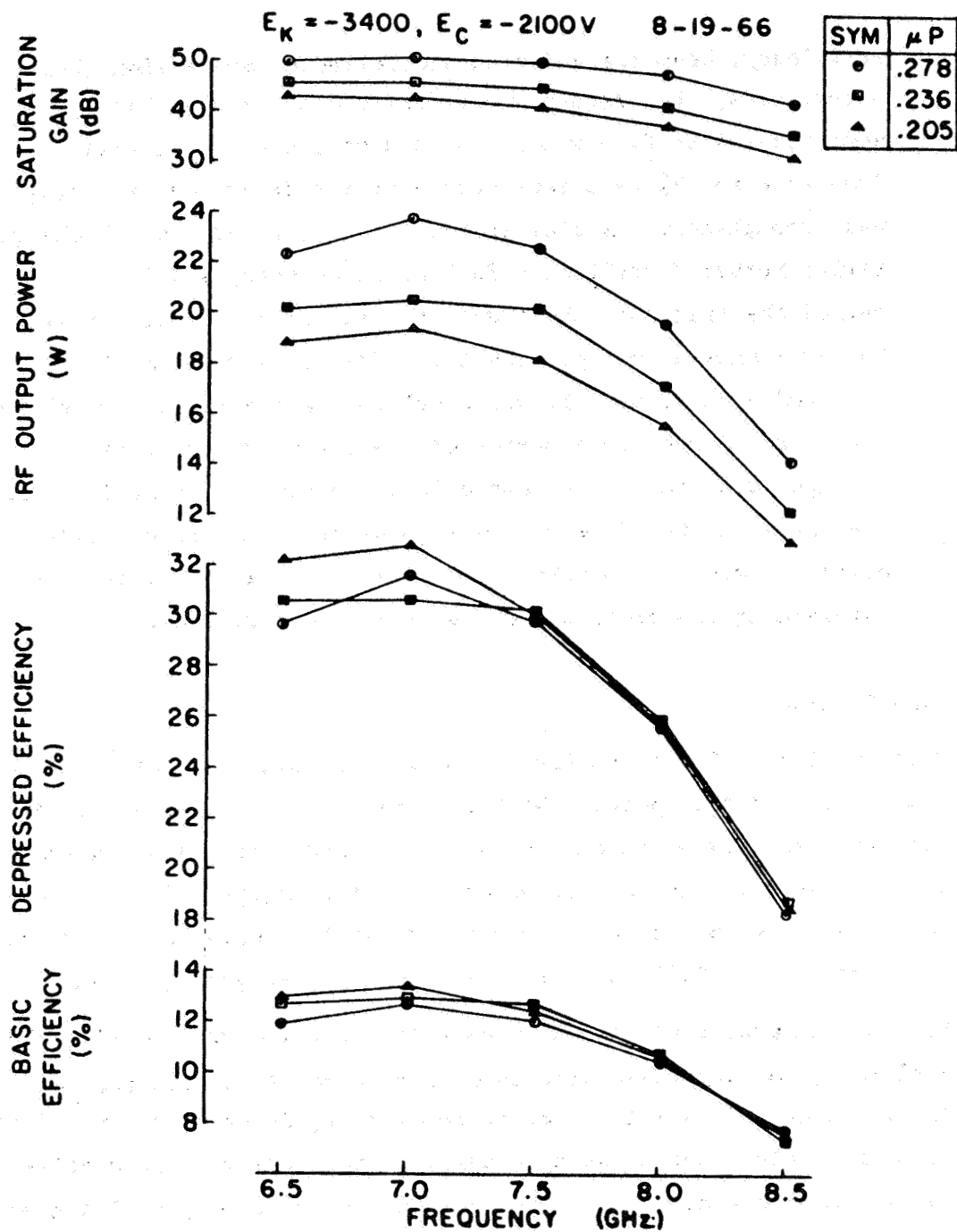


Figure 2 Power, efficiency and gain vs frequency for model 219H TWT, Serial Number 1.

| SERIAL NO. | 8 | 9 | 11 | 12 | 13 | 15 | 16 | 17 |
|-----------------------------------|-------|-------|-------|--------|-------|-------|--------|-------|
| MEASURED PARAMETERS: | | | | | | | | |
| BEAM MINIMUM DIAMETER | .0345 | .0400 | .0345 | .0345 | .0345 | .040 | .040 | .040 |
| MAGNETIC PERIOD | .480 | .480 | .480 | .270 | .270 | .270 | .270 | .270 |
| PEAK MAGNETIC FIELD | 1380 | 1350 | 1420 | 1800 | 1600 | 1600 | 1700 | 1700 |
| VOLTAGE FOR MAX SS GAIN | 3110 | 3110 | 3200 | 3200 | 3110 | 3325 | 3250 | 3250 |
| BASIC ELECTRO- NIC EFFICIENCY | 14.9% | 13.9% | 14.1% | 12.35% | 15.2% | 14.5% | 14.85% | 17.2% |
| ESTIMATED PARAMETER VALUES: | | | | | | | | |
| BEAM DIAMETER | .035 | .040 | .0339 | .0269 | .0302 | .0337 | .0317 | .0317 |
| % RIPPLE | 6.0 | 6.0 | 7.0 | <2.0 | <2.0 | <2.0 | <2.0 | <2.0 |
| $r_{b/o}$ | .543 | .620 | .526 | .417 | .468 | .523 | .492 | .492 |
| γ_o | 1.33 | 1.33 | 1.31 | 1.31 | 1.33 | 1.27 | 1.28 | 1.28 |
| γ_{r_b} (RELATIVE) | .722 | .825 | .688 | .546 | .622 | .664 | .629 | .629 |

DISTANCES = INCHES
MAGNETIC FIELD = GAUSS

Table 3 Beam parameters for model 219H TWT, second and third phase tubes.

A. Output Section Gain

Figure 3 shows the variation of basic efficiency with output section gain. The faired curve agrees with data recorded on an earlier X-band TWT design. The scatter in efficiency value for output section gain in excess of 26 dB is attributed to other efficiency-related variables discussed later in this report. For the purposes of this design, 26 dB has been determined to be the minimum allowable output section gain.

The actual length (gain) of the output section is limited by the VSWR of the internal attenuator and output connector. Any significant reflections at both of these points will tend to set up regenerative oscillation in the output section. Serial Number 14 had such an oscillation condition, attributed to a poor attenuator VSWR. This problem was eliminated by changing the internal attenuator loss pattern to reduce the attenuator VSWR.

B. Overvoltageing

Figure 4 demonstrates the typical variation of TWT performance parameters with cathode (beam) voltage. The term "overvoltage" refers to the increase in cathode to helix potential over the nearly synchronous or maximum small signal gain voltage. The "small signal gain voltage" is nominally 3275 V for this circuit configuration while the optimum operating helix-to-cathode voltage is nominally 3400 V. At this voltage, the maximum basic electronic efficiency has been achieved and operation at higher voltage tends to reduce the overall efficiency through degradation of the collector depression/beam transmission efficiency improvement factors. These results also are shown in Figure 4 .

MODEL 219-H TWT
S/N 'S AS NOTED

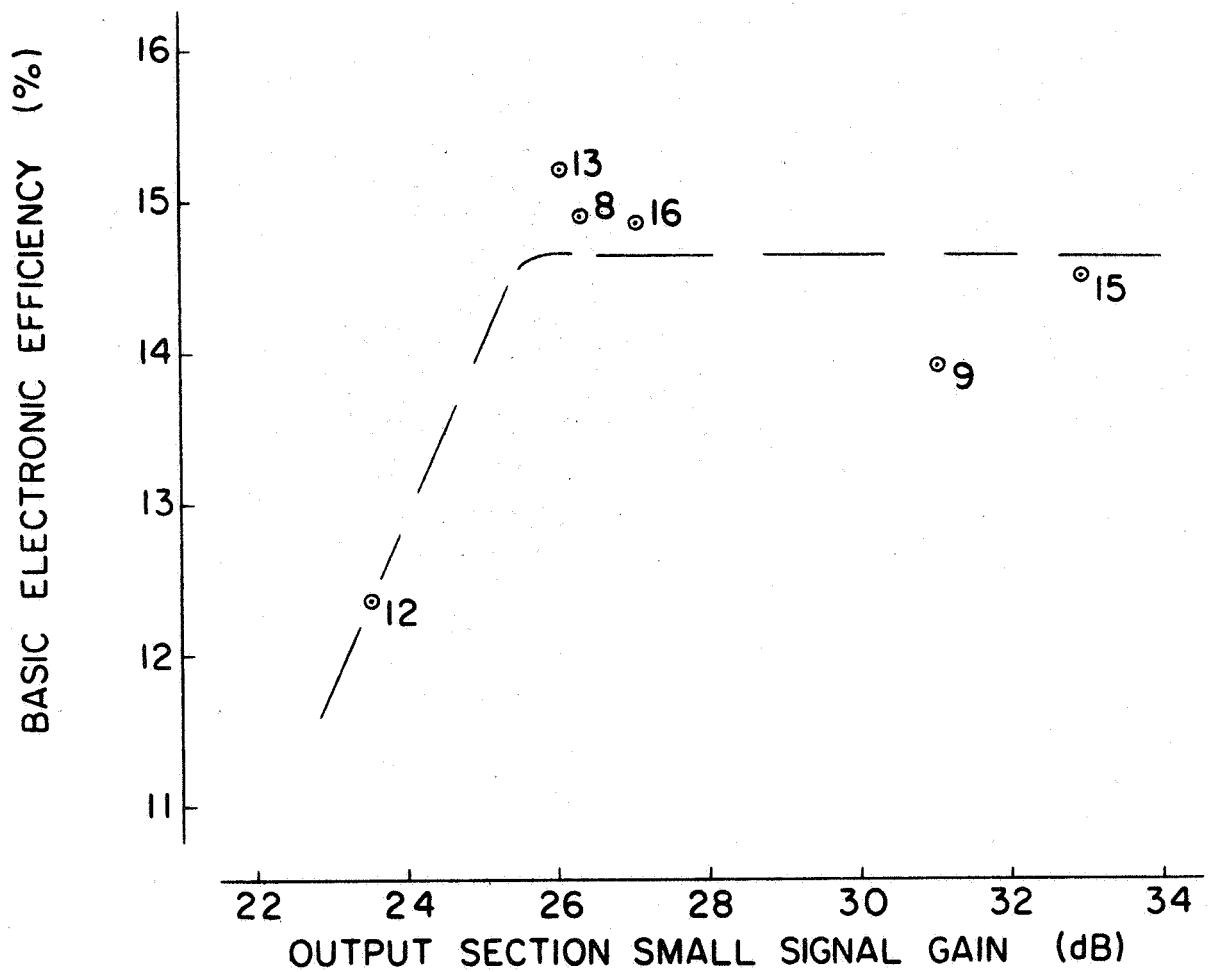


Figure 3 Basic efficiency vs output section small signal gain.

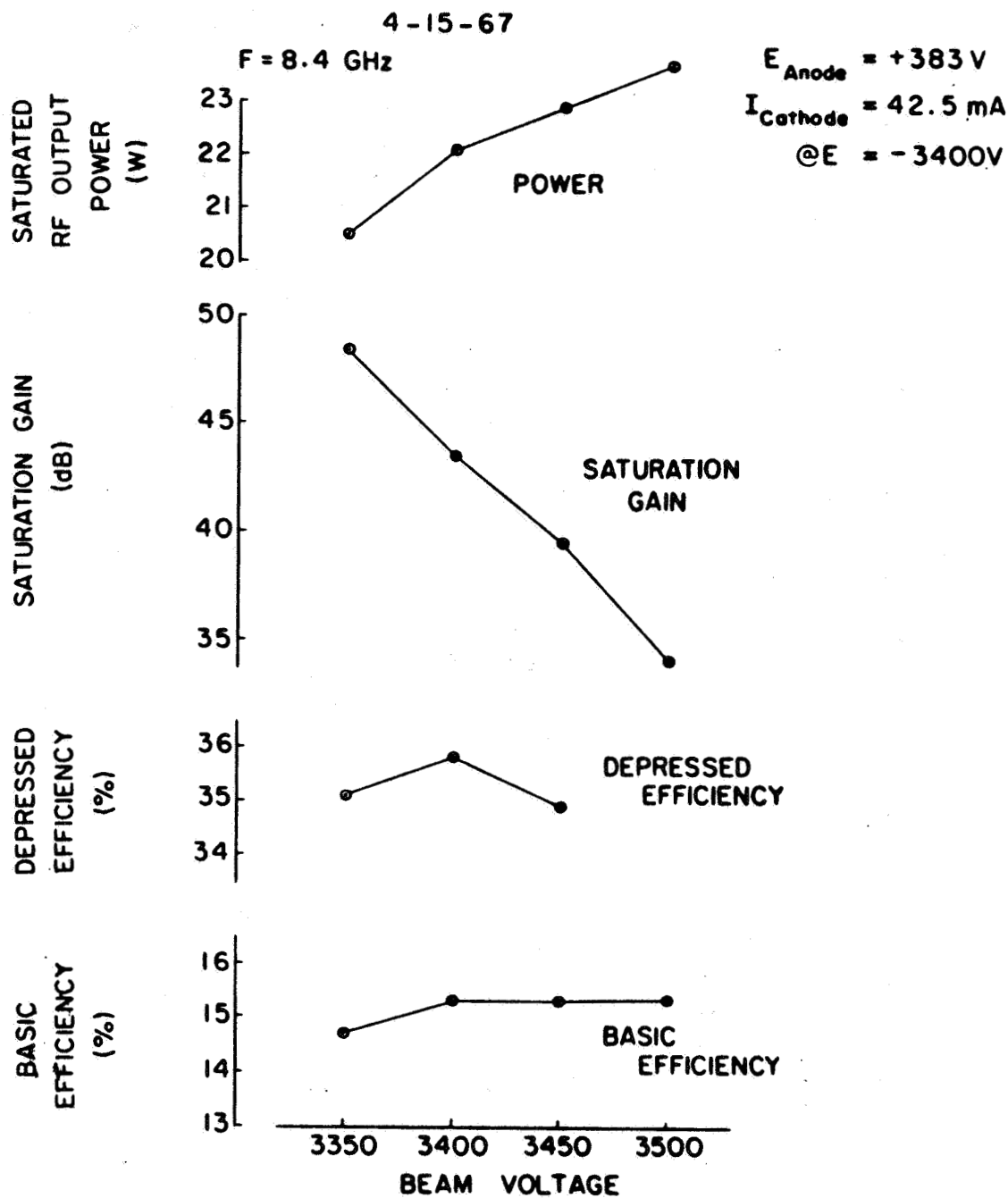


Figure 4 Power, gain and efficiency vs beam voltage for model 219H TWT, Serial Number 16.

C. Beam Diameter (γr_b)

Over a small range of values of the parameters QC and C, the basic electronic efficiency varies with the parameter γr_b in approximately the manner shown by the dashed lines in Figure 5. This data has been evaluated on several of the second phase tubes to ascertain the beam diameter for optimum basic efficiency. From this data it is apparent that optimum beam diameter can be achieved by utilizing the magnetic focusing field and beam minimum diameter values of Serial Number 13 or Serial Number 16 TWTS.

D. Collector Depression/Beam Transmission Efficiency Improvement Factor

For achieving maximum overall efficiency, the collector is operated at a depressed voltage (negative with respect to the helix). The amount of voltage depression is limited by the resulting degradation in beam transmission. Figure 6 shows the variation in helix current with collector depression voltage for saturation RF drive conditions. This shows that for values of collector depression in excess of 59% of the cathode voltage, the helix current tends to rise significantly. This is the limiting condition on collector depression.

The efficiency improvement factor is multiplied by the basic electronic efficiency to give the "depressed" electronic efficiency. Figure 7 plots the beam transmission vs collector depression for several values of the efficiency improvement factor (k). Figure 8 demonstrates the variation of achievable values of k with beam diameter, ($r_{b/a}$) for this collector design. Here it is seen that an optimum beam diameter exists. This is due to the variation in beam current density and hence in the space charge defocusing forces for low values of $r_{b/a}$ and the increasing beam diameter at high values of $r_{b/a}$.

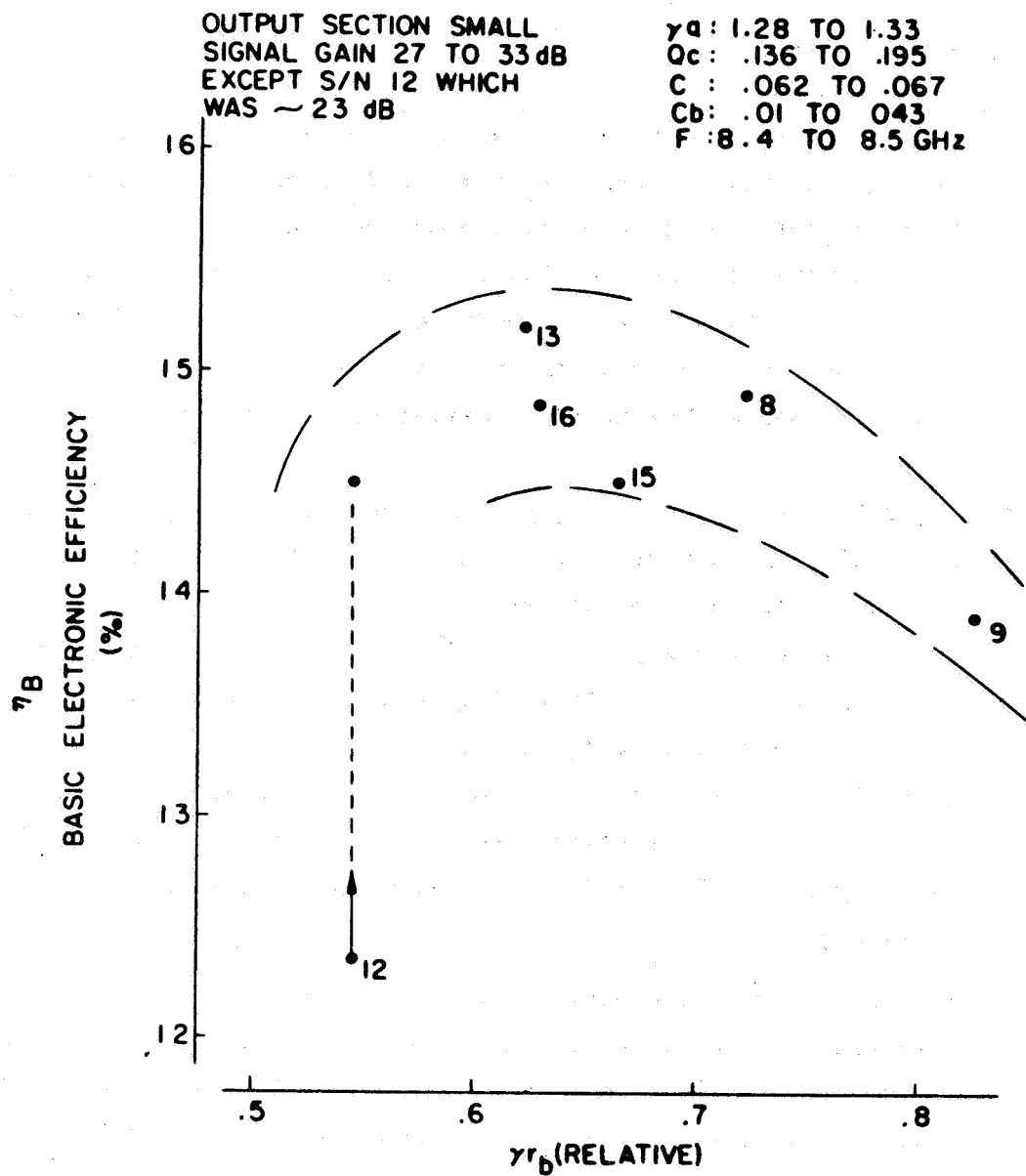


Figure 5 Basic efficiency vs γr_b parameter for model 219H TWT
Serial numbers as noted.

3-30-67
FIRST RF TEST

$E_K = -3400\text{ V}$
 $I_K = 42.6\text{ mA}$
 $P_{Out} = 21.0\text{ W (SAT)}$
 $F = 8.4\text{ GHz}$

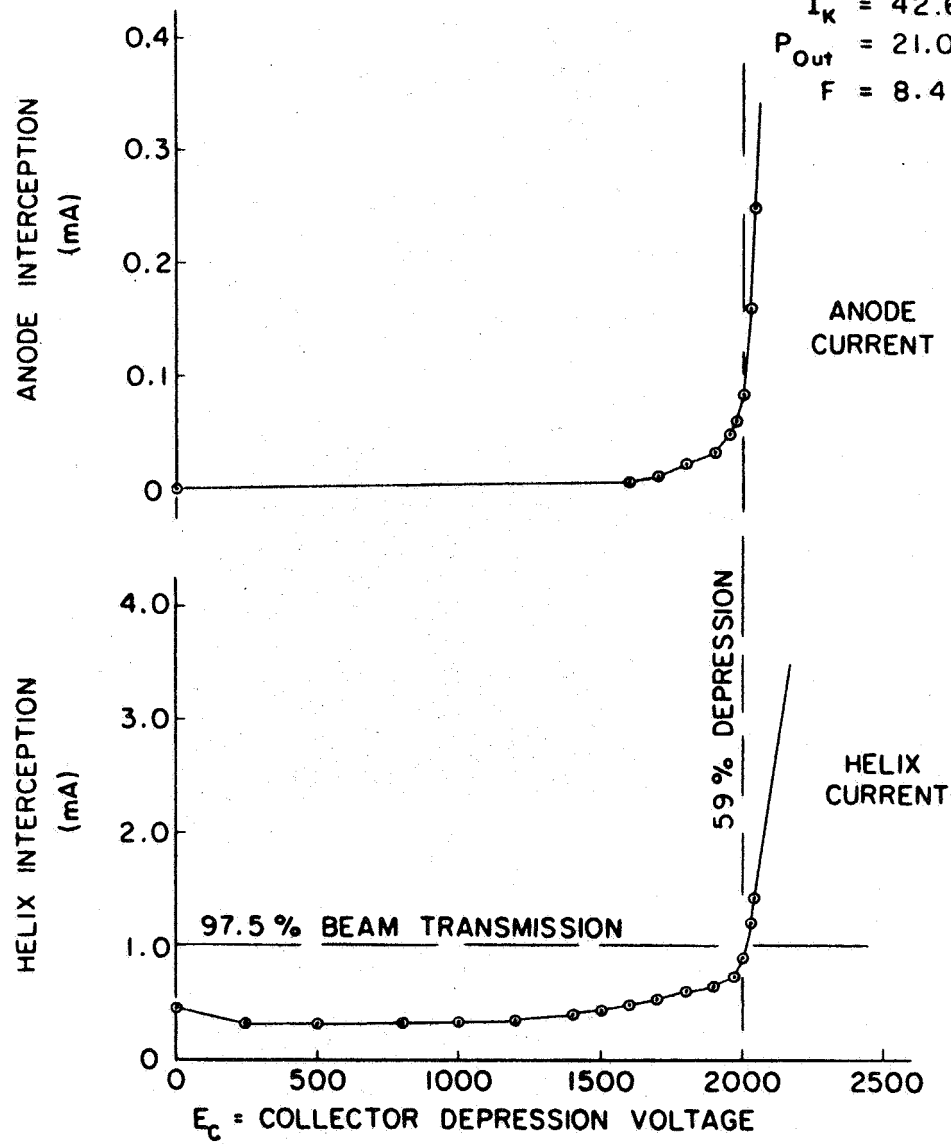


Figure 6 Helix and anode interception vs collector depression for model 219H TWT, Serial Number 16.

$$K = \frac{1}{1 - TD}$$

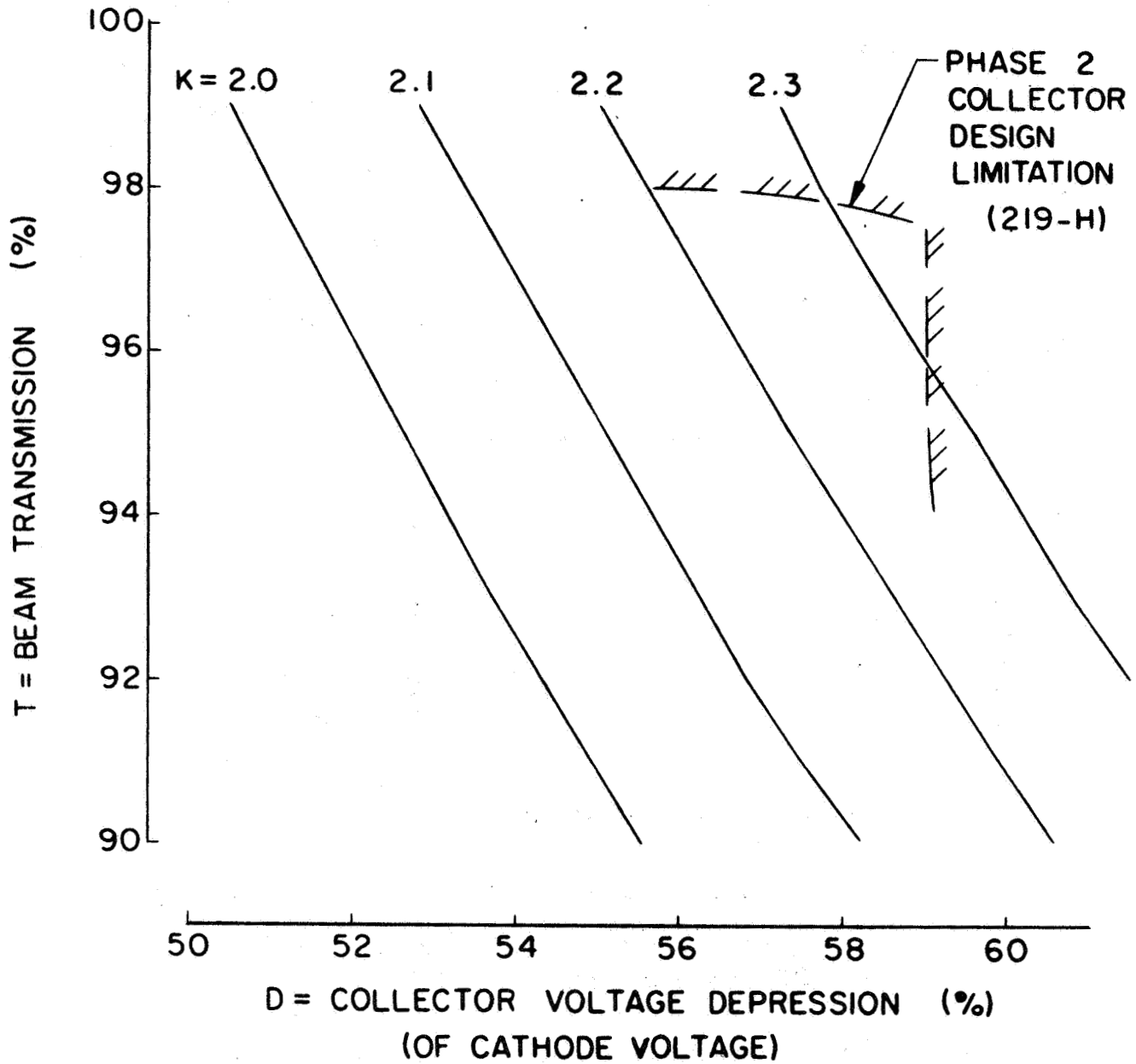


Figure 7 Beam transmission vs collector depression with electronic efficiency improvement factor as a parameter.

$$K \triangleq (1-TD)^{-1}$$

$T \triangleq$ % BEAM TRANSMISSION

$D \triangleq$ % COLLECTOR DEPRESSION

CIRCUIT LENGTH AND HELIX
DIMENSIONS HELD CONSTANT
COLLECTOR DIMENSIONS CONSTANT

NOMINAL $E_K = 3400V$

NOMINAL $I_K = 43mA$

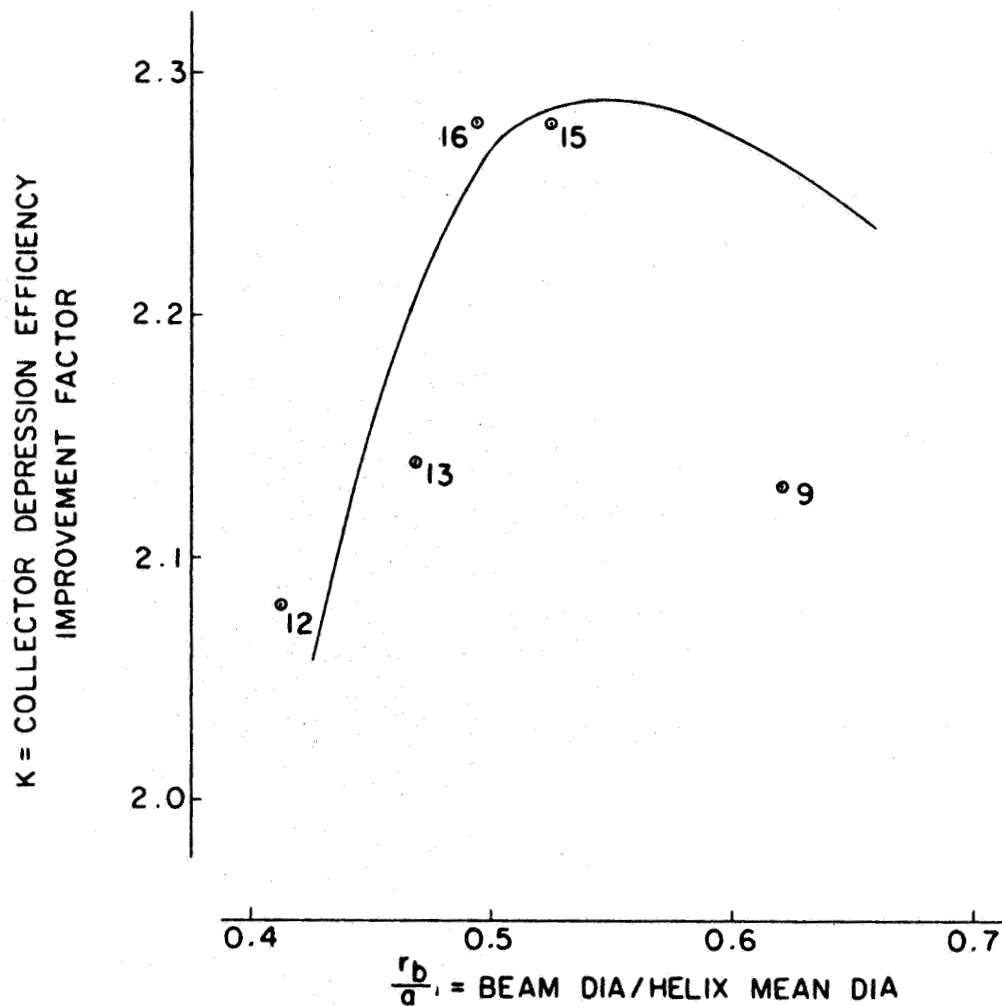


Figure 8 Collector depression efficiency improvement vs relative beam diameter for model 219H TWT, Serial Number noted.

E. Optimum Compromise Beam Configuration

Figure 9 presents a composite of the beam size related efficiency parameters together with the resultant overall electronic efficiency; all plotted against beam diameter. It may be seen that the best overall efficiency tends to occur somewhere between the values for maximum basic efficiency and maximum improvement factor. From this result, the gun and focusing field parameters from Serial Number 16 were chosen as a basis for further development.

Up to this point in the program, Serial Number 16 represented the best performance. Figure 10 shows key test results on Serial Number 16 as related to the specification values. The single shortcoming, at this juncture, is 2 to 3 "points" lacking in overall efficiency.

IV. THIRD PHASE

Two methods for further enhancement of efficiency were initiated. The first was copper plating of the helix and the barrel ID. The second was the redesign of the collector to a single and/or double stage bucket configuration. It was anticipated that one or a combination of these methods would provide the additional increment of efficiency required. The bucket collector has not been implemented in a TWT because the initial copper plated circuit tube provided the necessary increase in efficiency.

A. Copper Plated Slow Wave Structure

Serial Number 17 was constructed with a copper plated slow wave structure (both helix and barrel ID). The plating, a few ten thousands of an inch thick, and greater than the skin depth of copper at these frequencies, greatly reduced the resistive circuit losses. As a result, the basic efficiency and RF output power were considerably enhanced. Figure 11 compares Serial Number 17 to the second phase tubes on the basis of basic efficiency and efficiency improvement factor at comparable over-voltage conditions. Since the improved efficiency resulted in

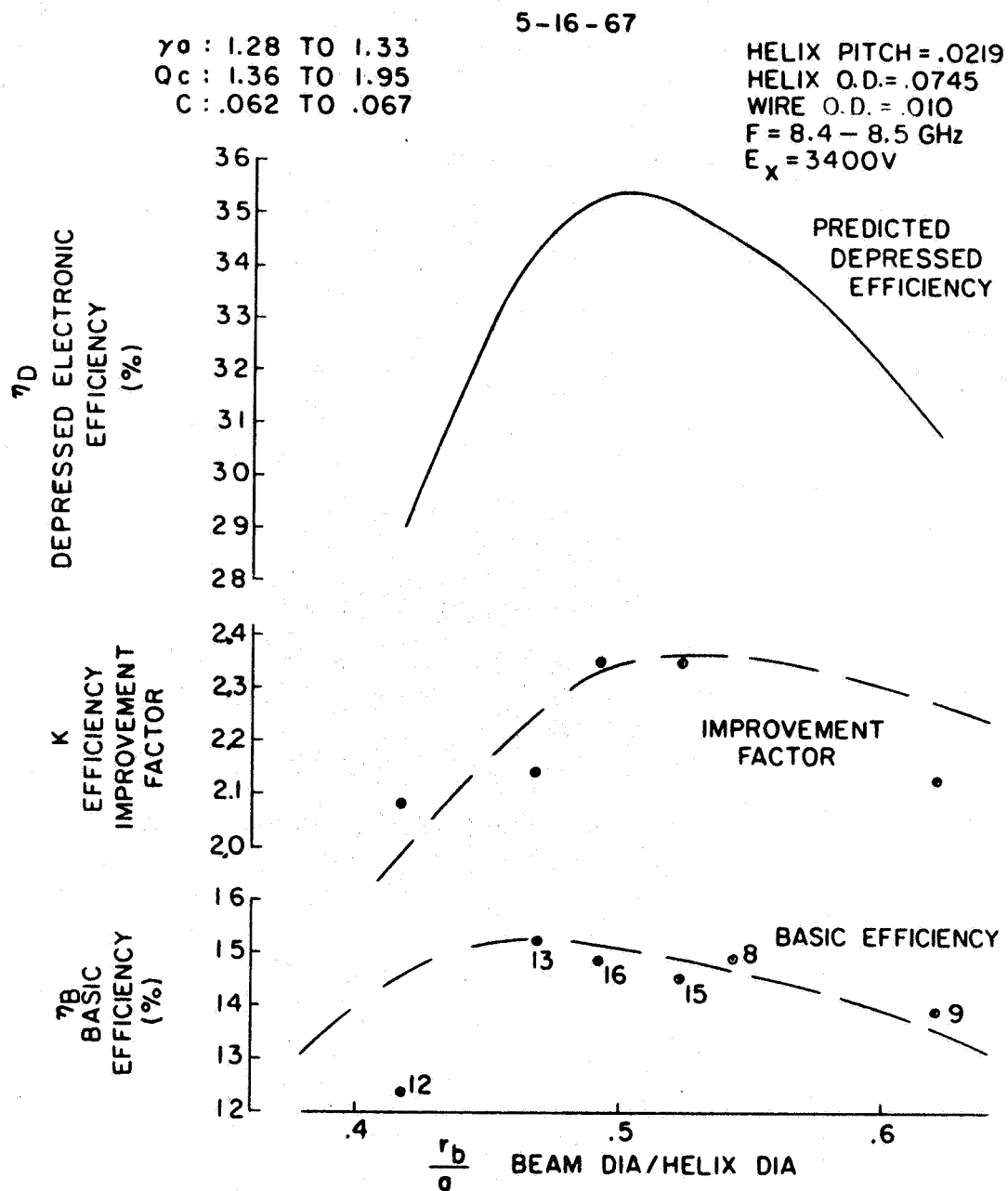


Figure 9 Efficiency parameters vs beam diameter for model 219H TWT, Serial numbers noted.

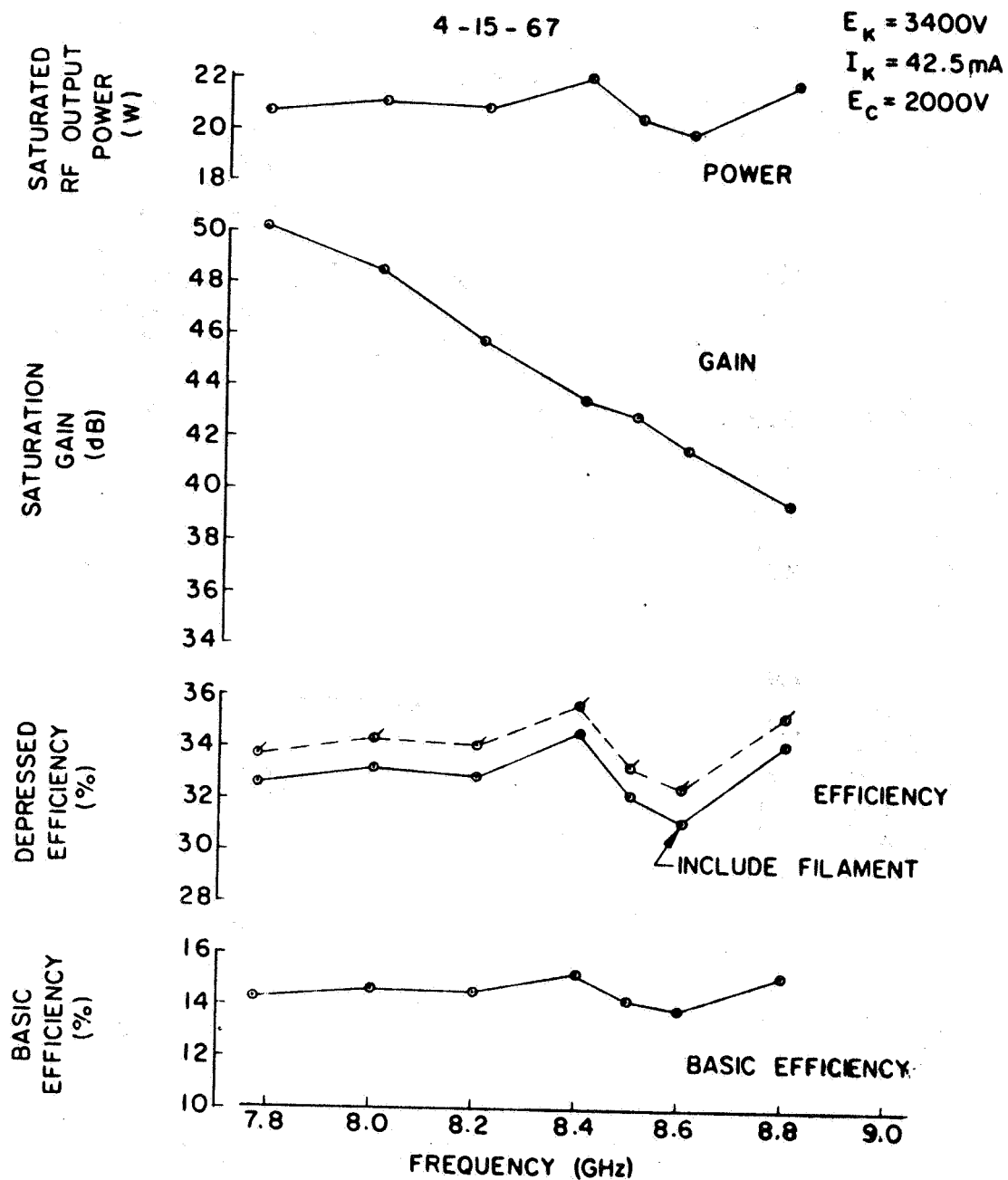


Figure 10

Power, gain and efficiency vs frequency for model 219H TWT, Serial Number 16.

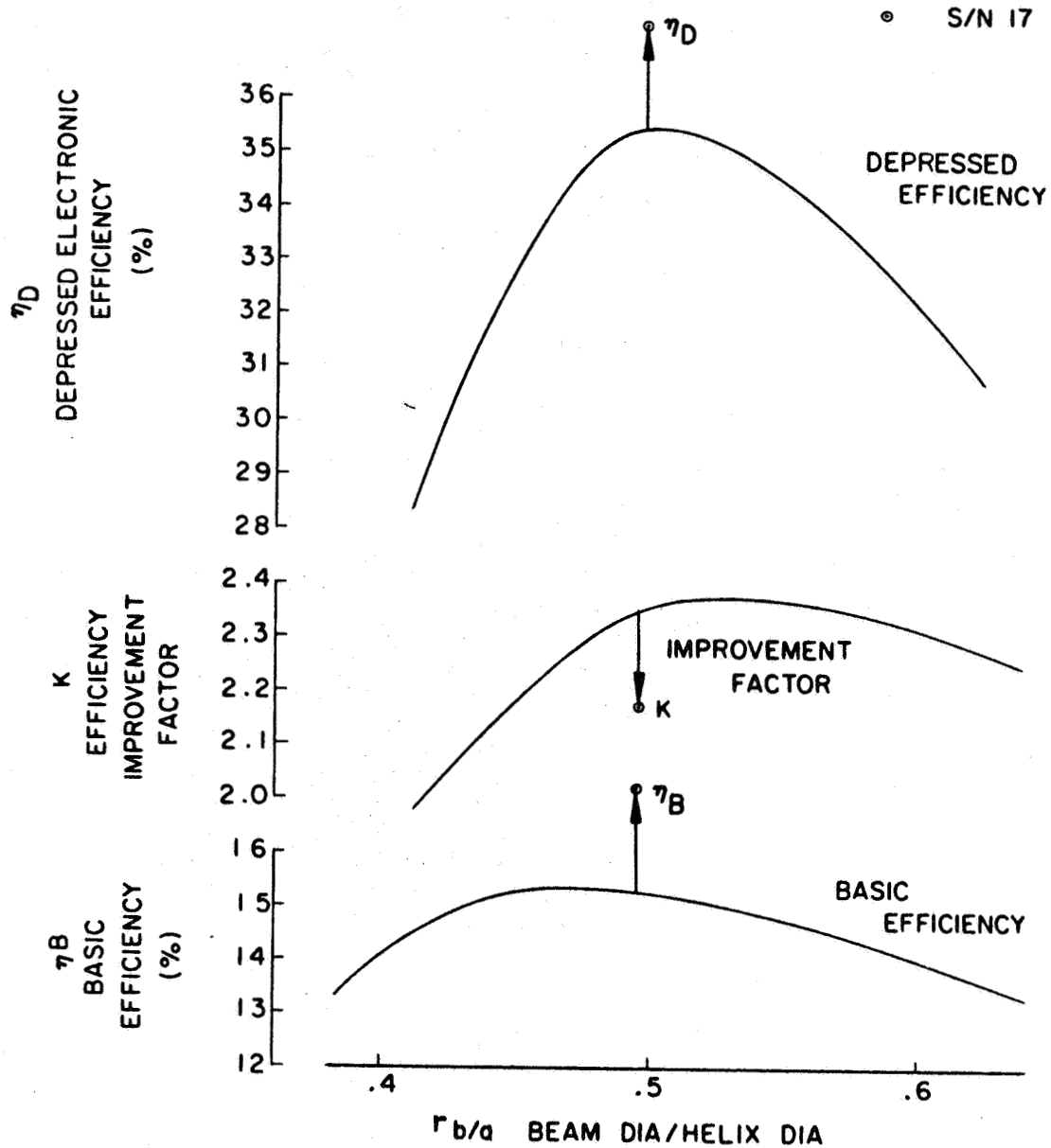


Figure 11 Efficiency parameter vs beam diameter for model 219H TWT, Serial Number 17 relative to phase 2 results.

excess RF output power, the TWT was out of specification at these conditions. Consequently, the voltages were reduced to bring the RF power down to the specified maximum while maintaining the specified efficiency. These results are shown in Figure 12.

B. TWT Performance

1. Power and Gain

Figure 12 and tables 4 and 5 show these parameters for two cases. Each case is defined as a particular set of operating voltages. Both cases demonstrate sufficient gain. Case 1 has excessive output power while for Case 2 the power is down in the specified range over the full 100 MHz band as well as the specified 10 MHz band within. Figures 13a, b, c, and d show RF output vs RF input power for Case 1 and 2 at 8.445 and 8.455 MHz.

2. Efficiency

Overall efficiency is also shown in Figure 12 and tables 4 and 5 for the two cases just mentioned. Here it is seen that for Case 1 the overall efficiency exceeds 35% over the 100 MHz band. For Case 2, the efficiency exceeds 35% over a 55 MHz band including the specified 10 MHz band for power performance. Higher power and efficiency have been demonstrated at different voltages. These results are given in a later section.

3. Bandwidth

The saturated power gain variation vs frequency is shown in Figures 14a, and b for the same two cases. The maximum gain slope is less than .010 dB/MHz.

7 - 20 - 67

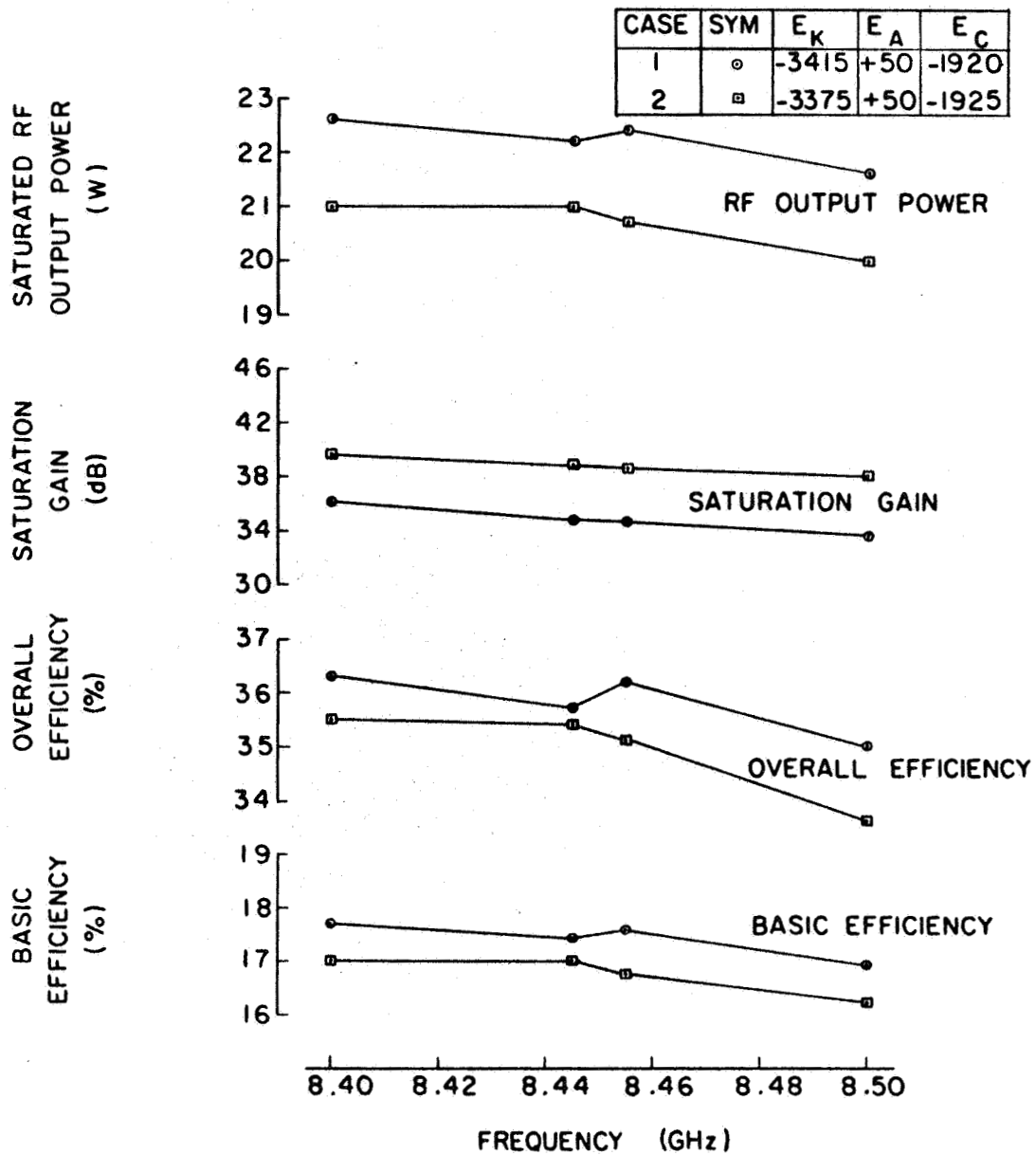


Figure 12 Power, gain and efficiency vs frequency for model 219H TWT, Serial Number 17.

OUTPUT POWER & EFFICIENCY DATA

TUBE TYPE 219 TESTED BY A.F. DATE 7-20
 TUBE NO. 17 ARM NO. 19813
 HEATER POWER E_f 45 I_f .269 = P_f 1.21 DATE CALIBRATED 7-14-67

| F | E_k | E_b | E_a | I_a | I_{tot} | η_B | I_w | I_b | P_w | P_p | P_b | P_{beam} | P_{tot} | P_{in} | P_{out} | η_D | η_{tot} | η_{gain} |
|-------|-------|-------|-------|-------|-----------|----------|-------|-------|-------|-------|-------|------------|-----------|----------|-----------|----------|--------------|---------------|
| 8.4 | 3415 | -1920 | +50 | .385 | 37.33 | 17.7 | 2.38 | 34.57 | 8.12 | 51.6 | 1.33 | 61.05 | 62.26 | 5.5 | 22.6 | 37.0 | 36.3 | 36.15 |
| 8.445 | 3415 | -1920 | +50 | .406 | 37.33 | 17.4 | 2.23 | 34.69 | 7.61 | 51.9 | 1.40 | 60.91 | 62.12 | 7.3 | 22.2 | 36.4 | 35.7 | 34.84 |
| 8.455 | 3415 | -1920 | +50 | .390 | 37.33 | 17.55 | 2.15 | 34.71 | 7.34 | 51.9 | 1.35 | 60.59 | 61.80 | 7.8 | 22.4 | 37.0 | 36.2 | 34.6 |
| 8.5 | 3415 | -1920 | +50 | .347 | | 16.9 | 2.1 | 34.86 | 7.18 | 52.2 | 1.2 | 60.58 | 61.79 | 9.5 | 21.6 | 35.7 | 35.0 | 33.6 |

SYMBOLS

F = Frequency (kHz)
 E_k = Cathode voltage with respect to helix
 E_b = Collector potential with respect to helix (volts)
 E_{1a} = First anode potential with respect to helix (volts)
 E_{2a} = Second anode potential with respect to helix (volts)
 I_{1a} = First anode current (mA)
 I_{2a} = Second anode current (mA)
 I_{tot} = Total cathode current (mA)
 E_f = Heater voltage (volts)
 I_f = Heater current (amps)
 I_w = Helix current (mA)
 I_b = Collector current (mA)
 P_w = Helix Power (watts)
 P_b = Collector power (watts)
 P_{tot} = Total dc power including heater power (watts)
 P_{beam} = Total dc power excluding heater power (watts)
 P_{in} = RF power input (mW)
 P_{out} = RF power output (watts)
 P_f = Heater power
 η_D = Beam efficiency (Depressed)
 η_{tot} = Total Efficiency
 P_A = Anode Power (watts)

Table 4

OUTPUT POWER & EFFICIENCY DATA

TUBE TYPE 219 TESTED BY A.F. DATE 7-17-67
TUBE NO. 17 ARM NO. 198.13 DATE CALIBRATED 7-14-67
HEATER POWER E_f 4.5 I_f .269 = P_f 1.21

| F | E_k | E_b | E_o | I_o | I_{tot} | η_B | I_w | I_b | P_w | P_p | P_o | P_{beam} | P_{tot} | P_{in} | P_{out} | η_D | η_{tot} | η_{sol} |
|-------|-------|-------|-------|-------|-----------|----------|-------|-------|-------|-------|-------|------------|-----------|----------|-----------|----------|--------------|--------------|
| 8.4 | 3375 | -1925 | +50 | .36 | 36.66 | 17.0 | 2.2 | 34.1 | 7.42 | 49.4 | 1.23 | 58.05 | 59.26 | 2.31 | 21.0 | 36.2 | 35.5 | 39.6 |
| | | | | | | | | | | | | | | | | | | |
| 8.445 | 3375 | -1925 | +50 | .367 | 36.66 | 17.0 | 2.2 | 34.10 | 7.42 | 49.4 | 1.26 | 58.08 | 59.29 | 2.7 | 21.0 | 36.1 | 35.4 | 38.92 |
| | | | | | | | | | | | | | | | | | | |
| 8.455 | 3375 | -1925 | +50 | .335 | 36.66 | 16.75 | 2.09 | 34.2 | 7.06 | 49.6 | 1.14 | 57.80 | 59.01 | 2.8 | 20.70 | 35.9 | 35.1 | 38.7 |
| | | | | | | | | | | | | | | | | | | |
| 8.5 | 3375 | -1925 | +50 | .370 | 36.66 | 16.20 | 2.33 | 33.98 | 7.87 | 49.2 | 1.27 | 58.34 | 59.55 | 3.18 | 20.0 | 34.3 | 33.6 | 38.0 |
| | | | | | | | | | | | | | | | | | | |

SYMBOLS

F = Frequency (kMc)
 E_k = Cathode voltage with respect to helix
 E_b = Collector potential with respect to helix (volts)
 E_{1a} = First anode potential with respect to helix (volts)
 E_{2a} = Second anode potential with respect to helix (volts)
 I_{1a} = First anode current (mA)
 I_{2a} = Second anode current (mA)
 I_{tot} = Total cathode current (mA)
 E_f = Heater voltage (volts)
 I_f = Heater current (amps)
 I_w = Helix current (mA)
 I_b = Collector current (mA)
 P_w = Helix Power (watts)
 P_b = Collector power (watts)
 P_{tot} = Total dc power including heater power (watts)
 P_{beam} = Total dc power excluding heater power (watts)
 P_{in} = RF Power input (mW)
 P_{out} = RF power output (watts)
 P_f = Heater power
 η_D = Beam efficiency (Depressed)
 η_{tot} = Total efficiency
 P_A = Anode Power (watts)

Table 5

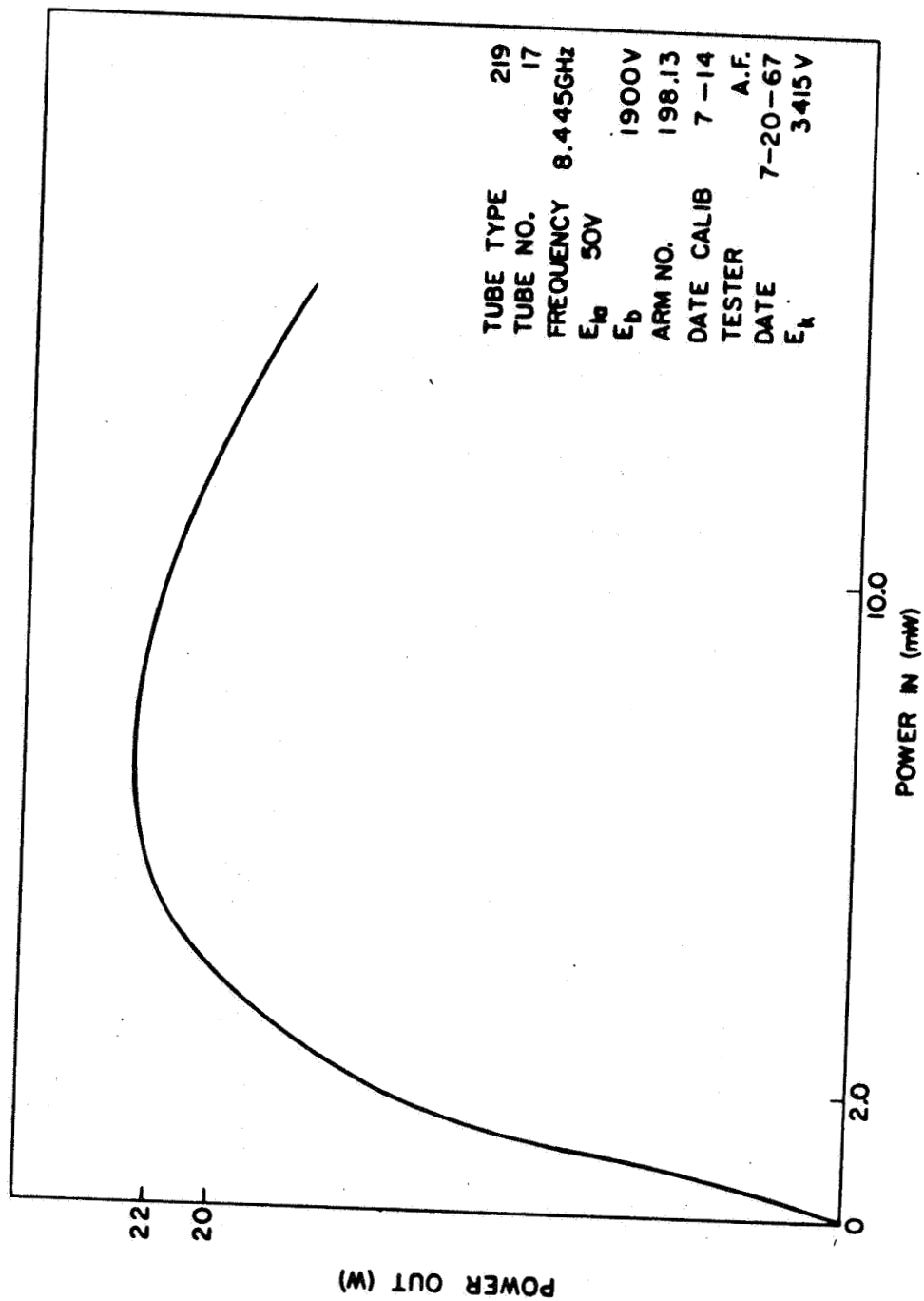


Figure 13A Power output vs power input.

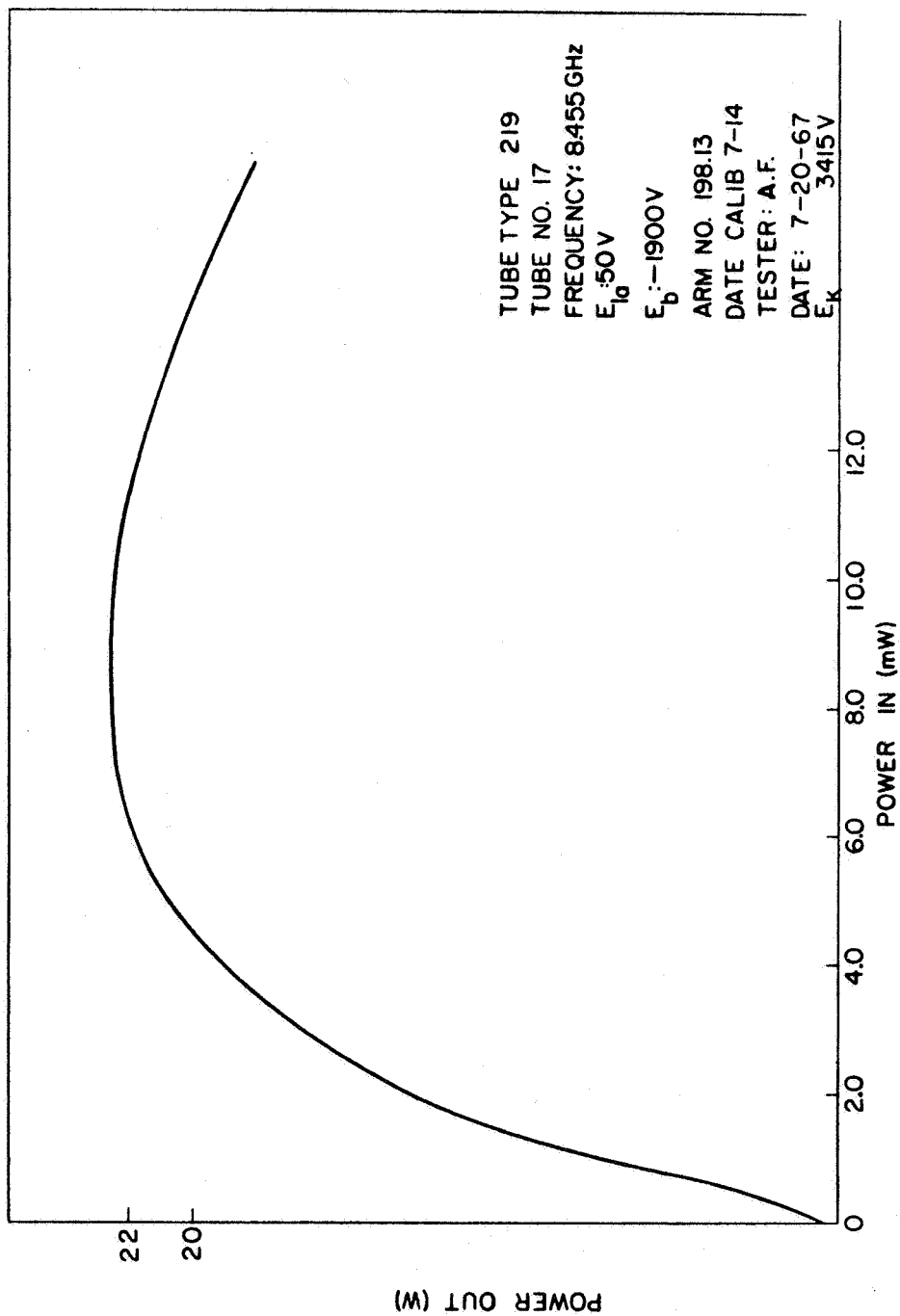


Figure 13B Power output vs power input.

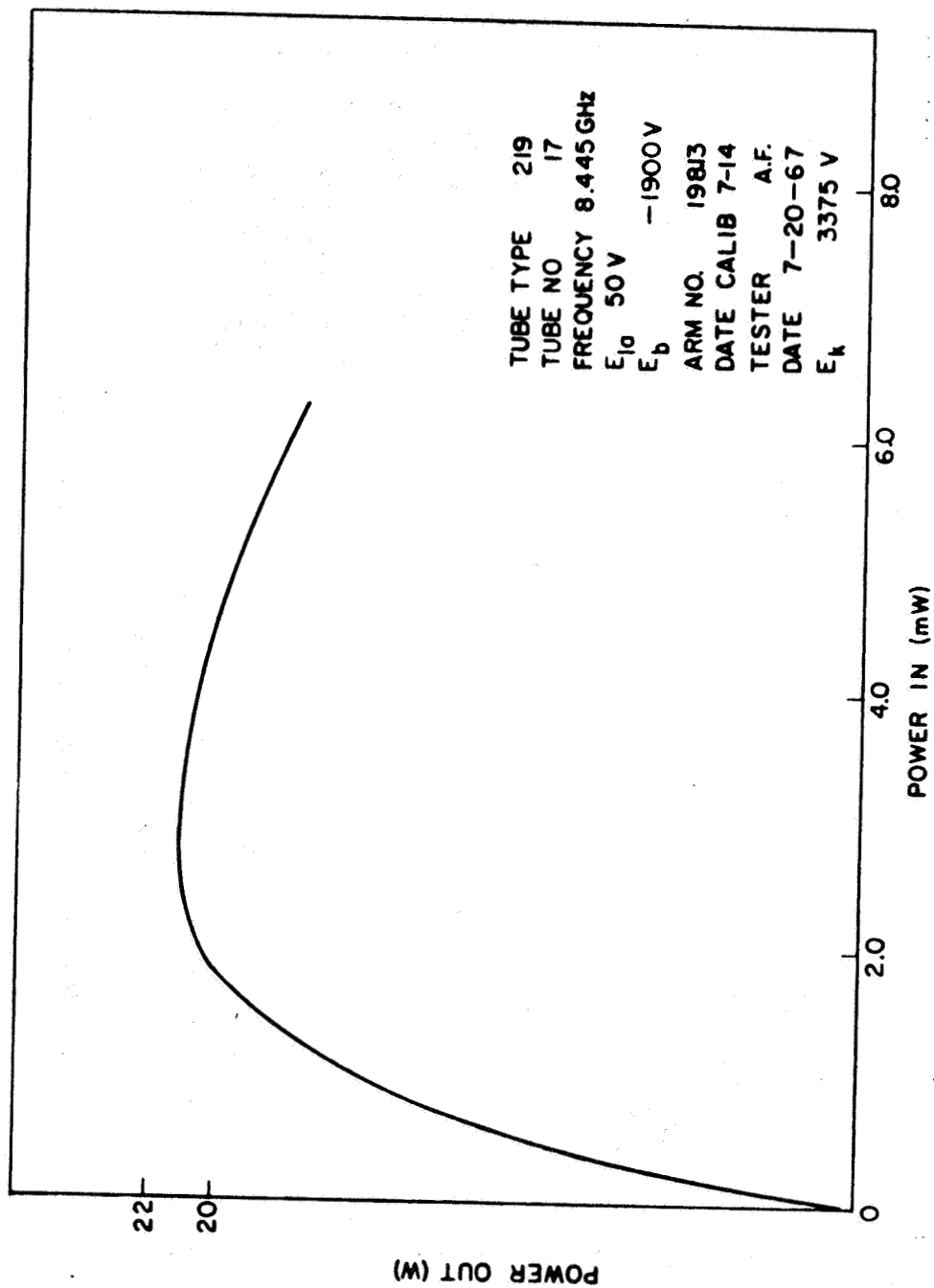


Figure 13C Power output vs power input.

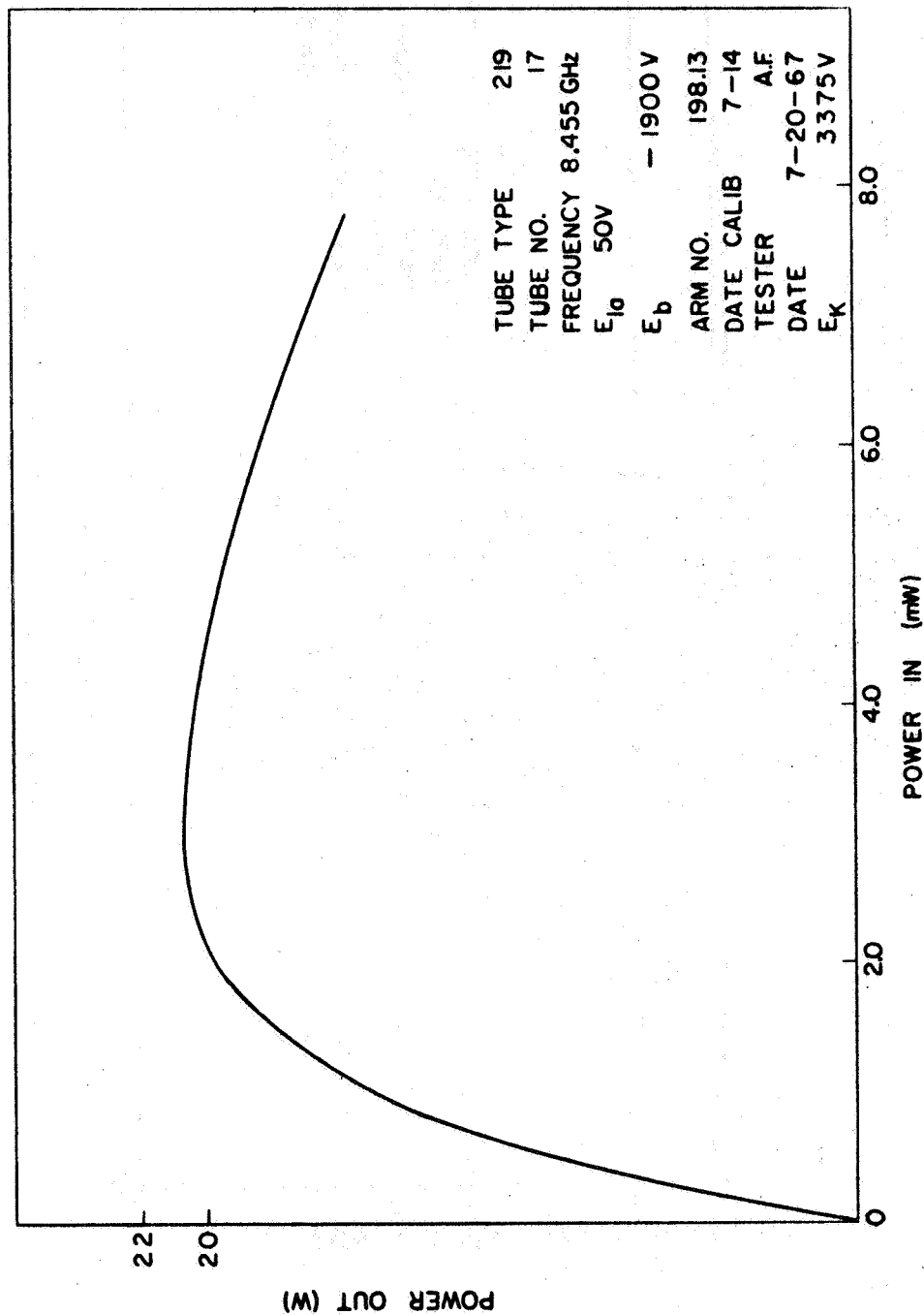


Figure 13D Power output vs power input.

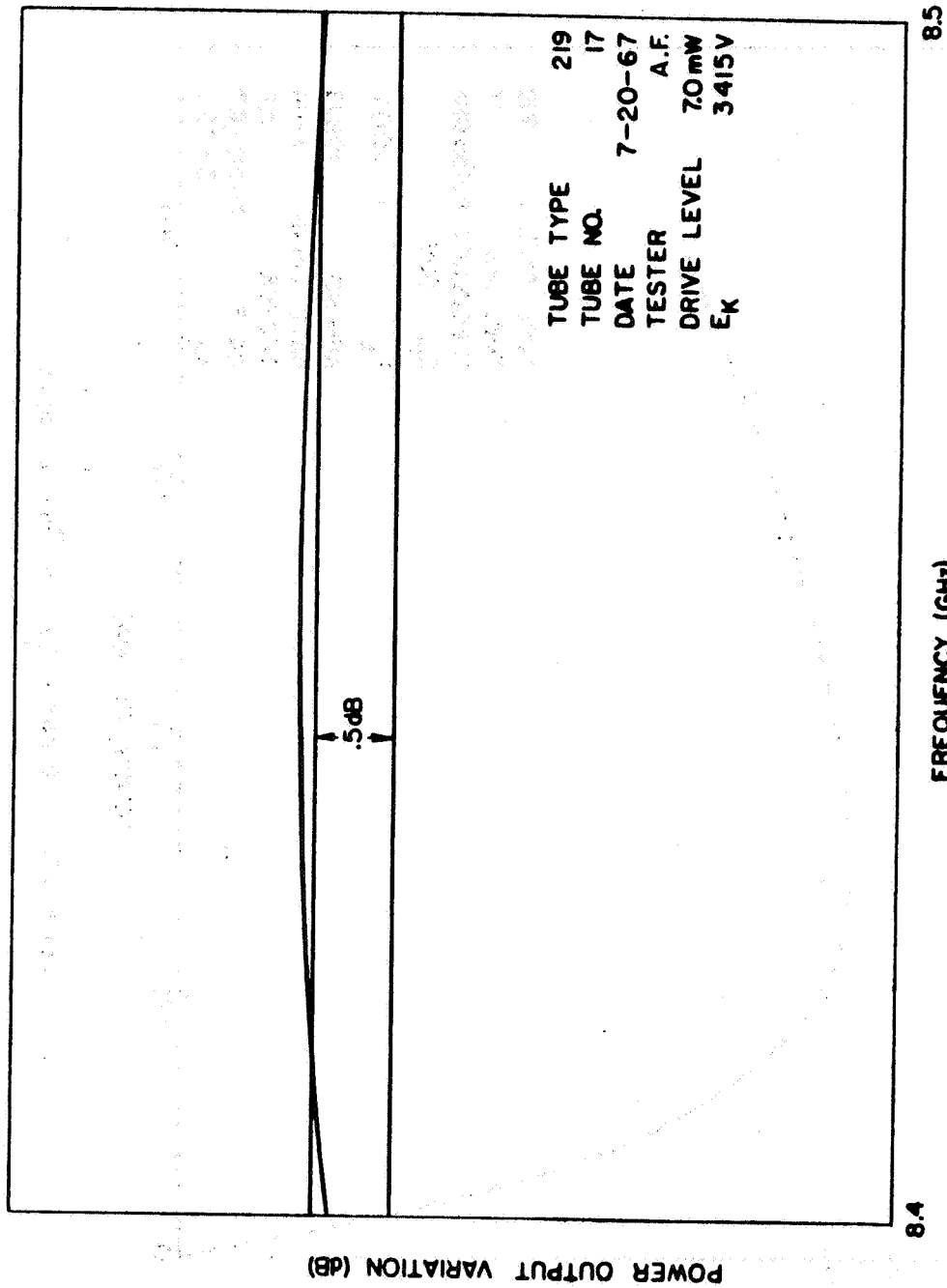


Figure 14A Saturated power variation vs frequency.

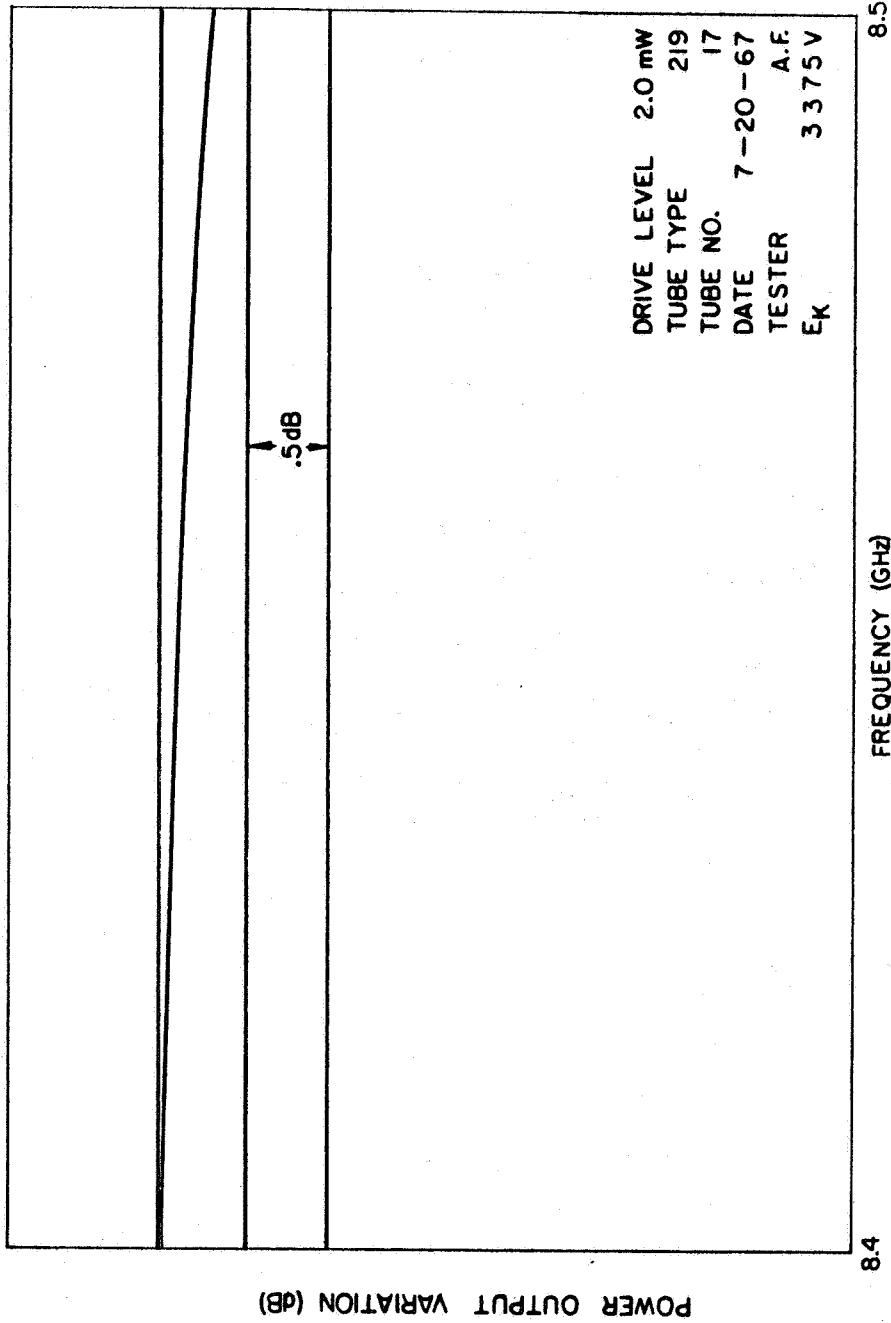


Figure 14B Saturated power variation vs frequency.

4. Noise Figure

The noise figure as measured on Serial Number 17 is 27.65 dB. The measurement was made at 8.4 GHz.

5. Impedance and Reflection Coefficient

Input and output RF connector impedance is 50 ohms. The input and output voltage reflection coefficients, recorded with the tube operating, are shown in Figure 15. A value of 20% for the voltage reflection coefficient is equivalent to a VSWR of 1.5:1.

6. Optimum Power and Efficiency

Serial Number 17, with reduced circuit loss, demonstrated enhanced power and efficiency with overvoltage. Figures 16 and 17 show the results of increased overvoltage at 8.4 and 8.8 GHz respectively. Here power, gain, and efficiency are plotted against beam voltage. Up to 27.5 watts of RF output power with 40.9% overall efficiency are demonstrated.

7. Phase Sensitivity

Figure 18 shows the change in phase through the tube due to a change in beam voltage. It is seen that the phase sensitivity is nominally 1 degree per volt.

8. Second (and Higher) Harmonic

Second (and higher) harmonic output power was measured on Serial Number 13 for a fundamental RF drive at 8.4 GHz. The maximum harmonic power was 330 mW, 18 dB down from the fundamental output level of 21 watts for the existing test conditions. Fundamental power is eliminated from harmonic power

HOT MATCH TUBE TYPE 219 $E_A = 50$ TESTER A.F.
 TUBE NO 17 $E_K = 3375$ DATE 7-20-67

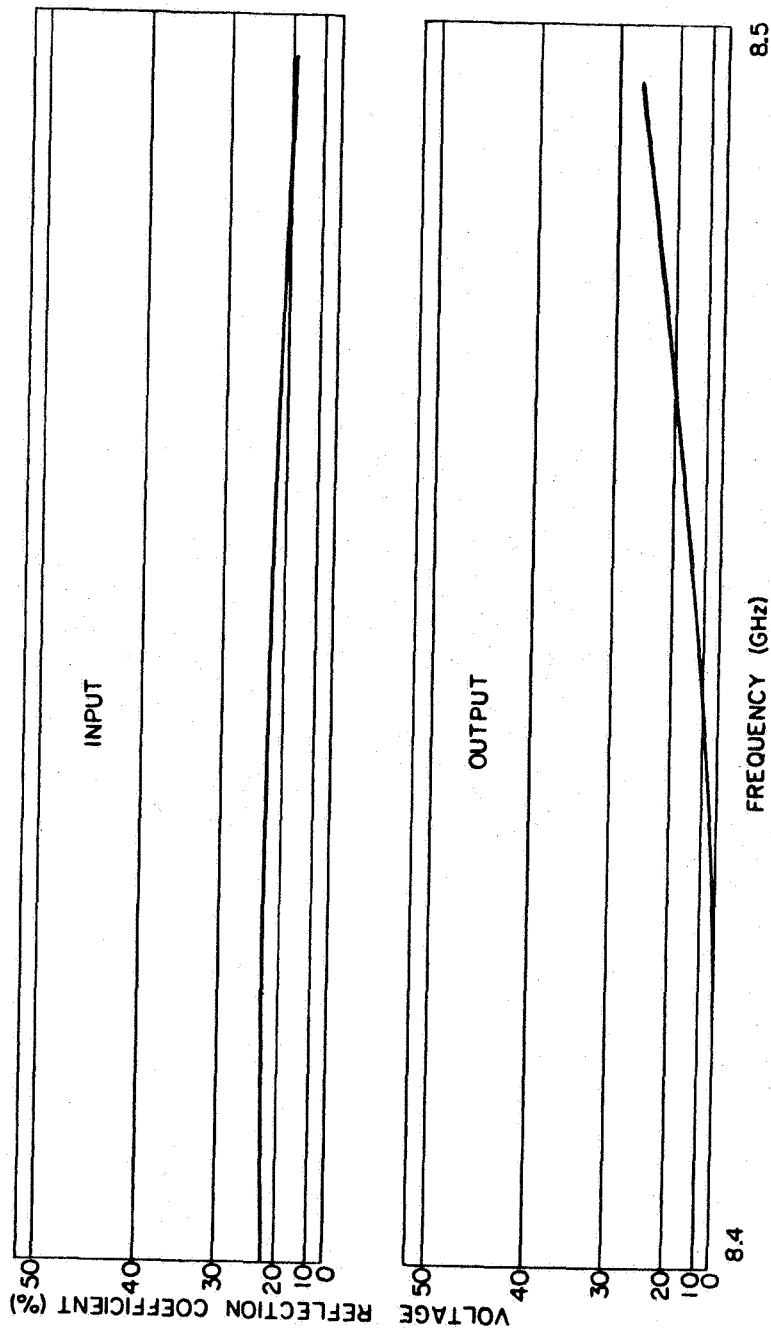


Figure 15 Hot output and hot input match vs frequency.

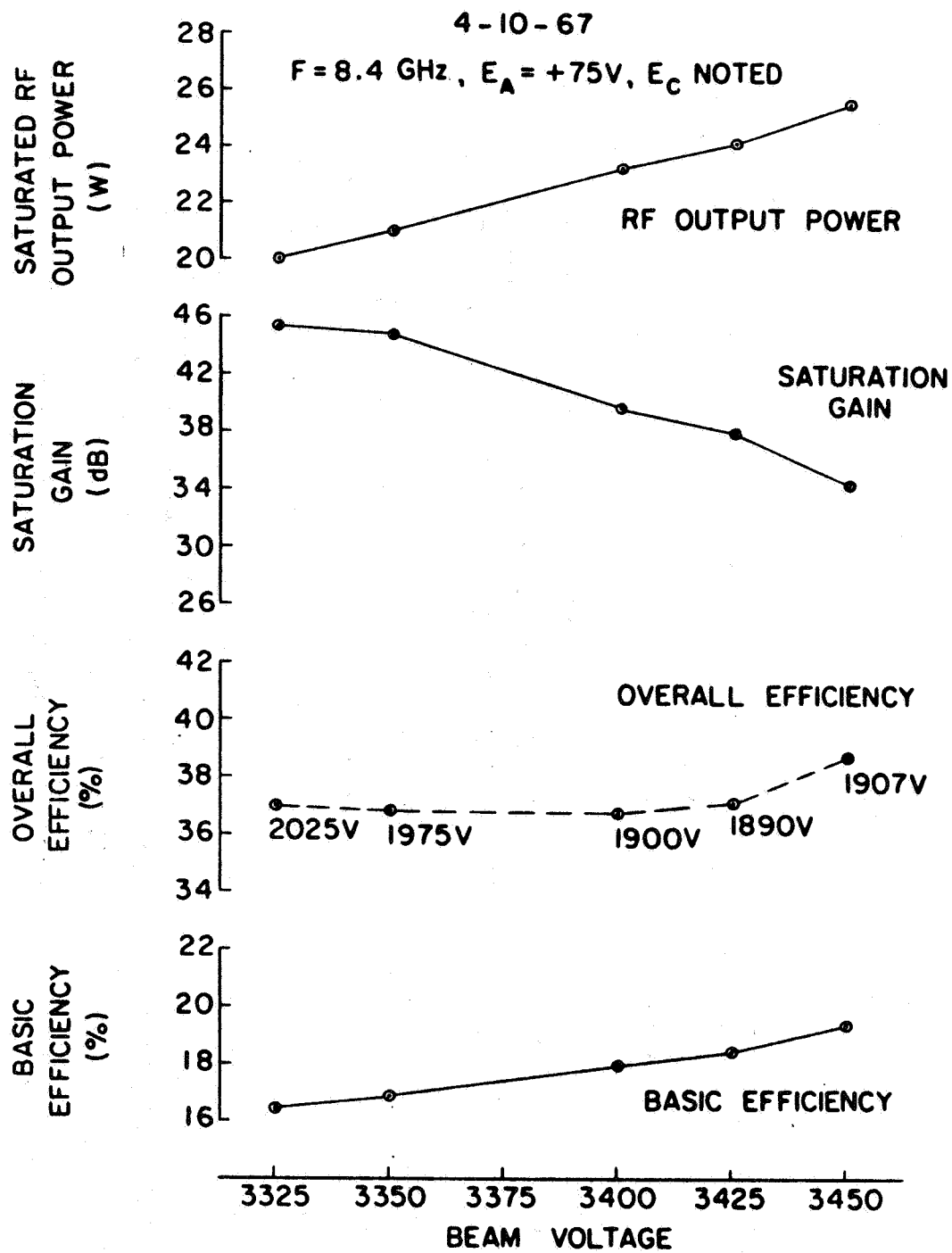


Figure 16 Power, gain and efficiency vs beam voltage for model 219H TWT, Serial Number 17.

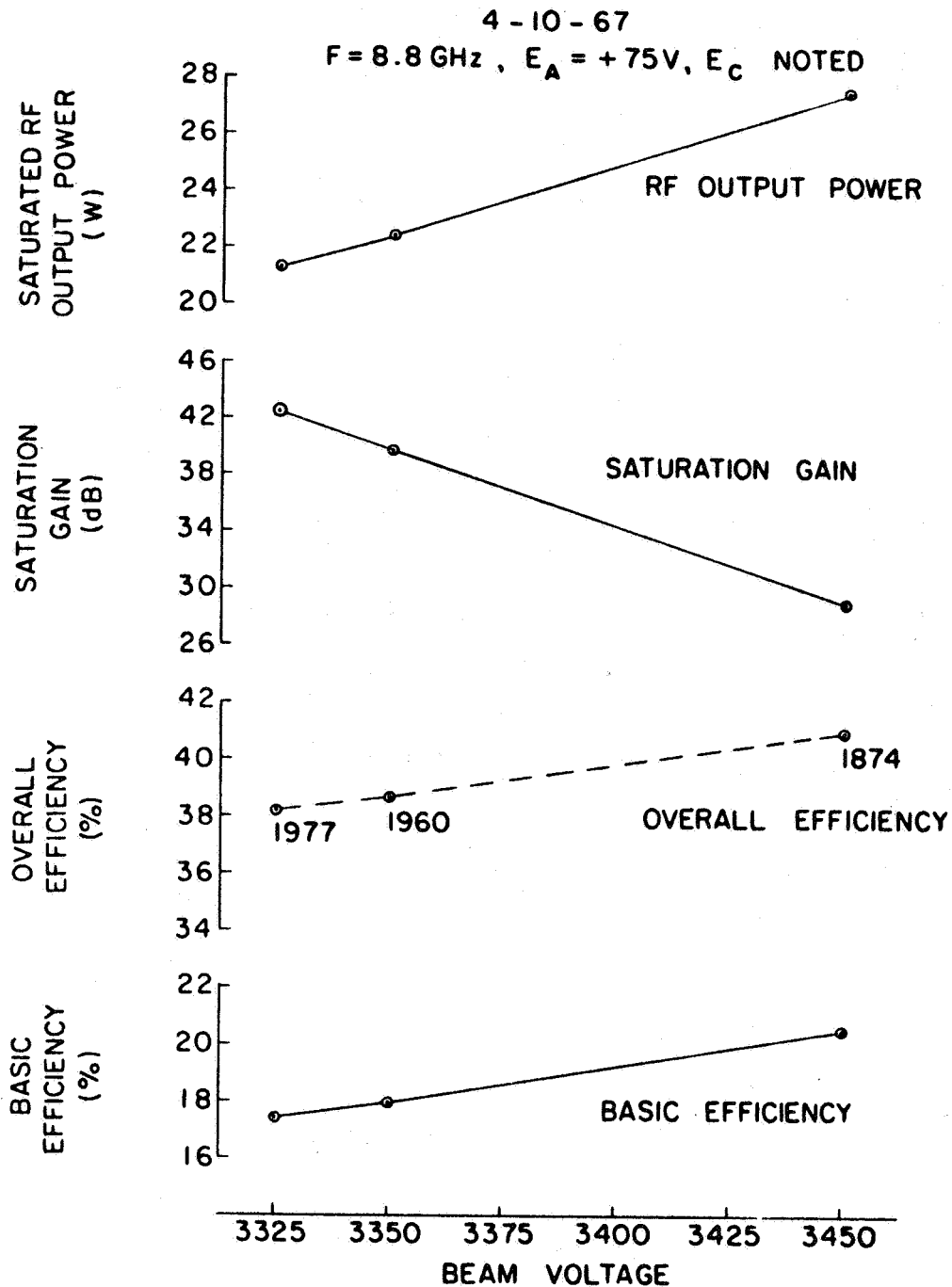


Figure 17 Power, gain and efficiency vs beam voltage for model 219H TWT, Serial Number 17.

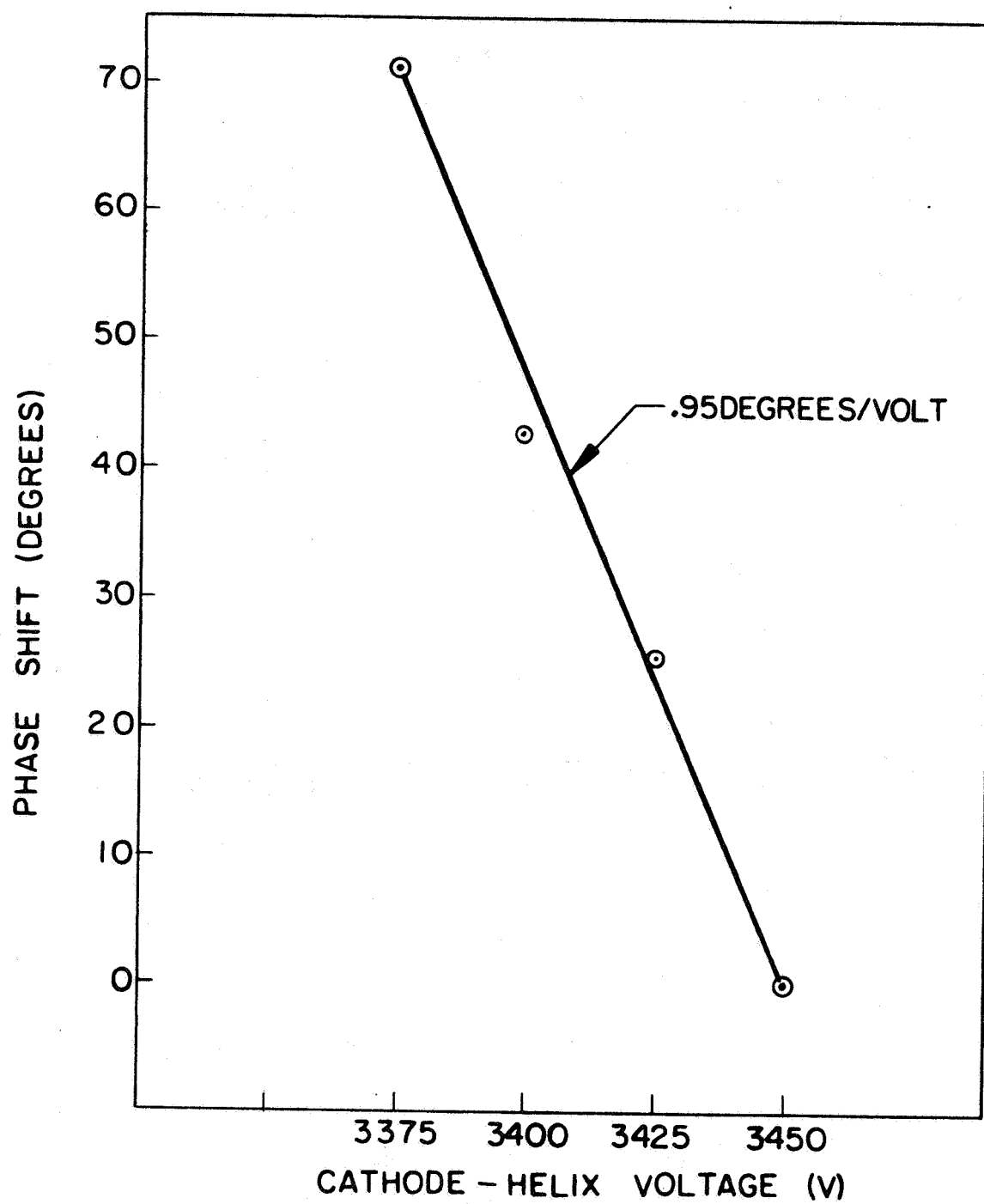


Figure 18 Phase shift vs helix voltage for model 219H TWT, Serial Number 1.

measurements by inclusion of a high pass filter (waveguide which cuts off between fundamental and second harmonic) in the calibrated measuring arm. Similarly second harmonic power is eliminated from all fundamental power measurements by inclusion of a 10 GHz low pass filter in the calibrated measuring arm.

POWER SUPPLY

Introduction

The purpose of this section of the final report is to discuss in detail the design approach used by Engineered Magnetics for the power supply.

Since Engineered Magnetics has already designed many traveling-wave tube power supplies specifically for satellite application, the following discussion describes an approved circuit design, rather than a new design approach.

Circuit Description

The sub-circuits discussed in the circuit description are shown in the block diagram, Figure 19, and in the schematic, Figure 20.

Voltage Regulator

The input voltage regulator is a fixed frequency, variable duty cycle circuit (pulse-width regulator). This type of regulator was selected because of the following advantages:

High efficiency over a very wide range of input voltages, typically 95 - 96% at 24 volts, and 94% at 32 volts.

Tight regulation, typically 50 mV change in the output voltage level of 22 volts, with an input change of 8 volts.

High attenuation of input ripple, typically 40 dB.

Circuit simplicity.

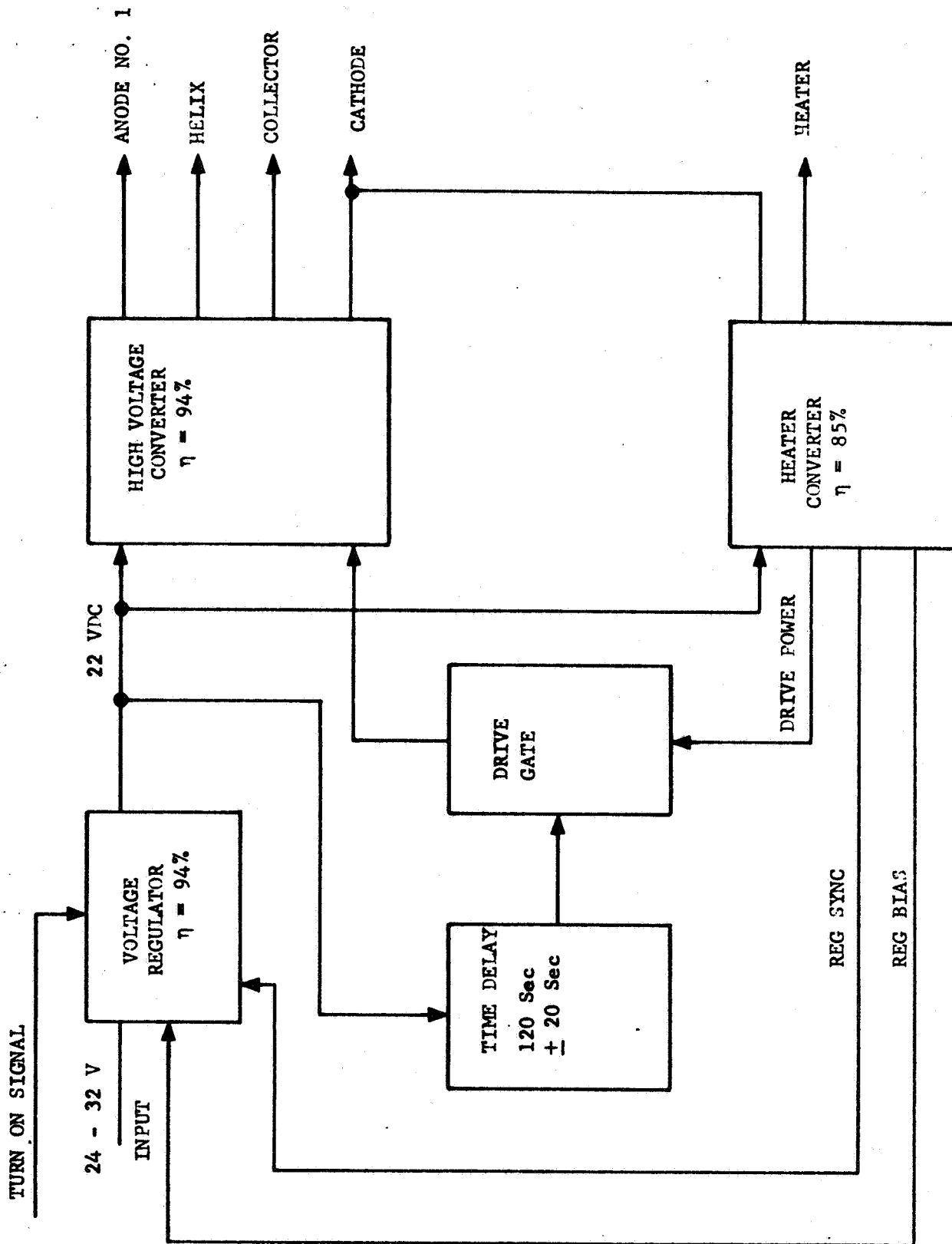
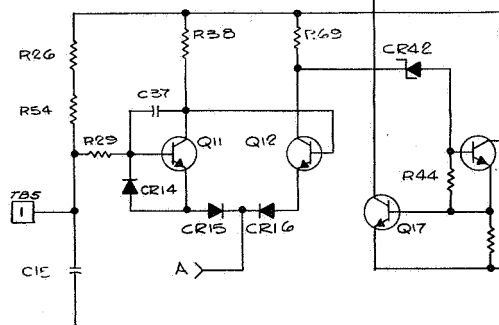
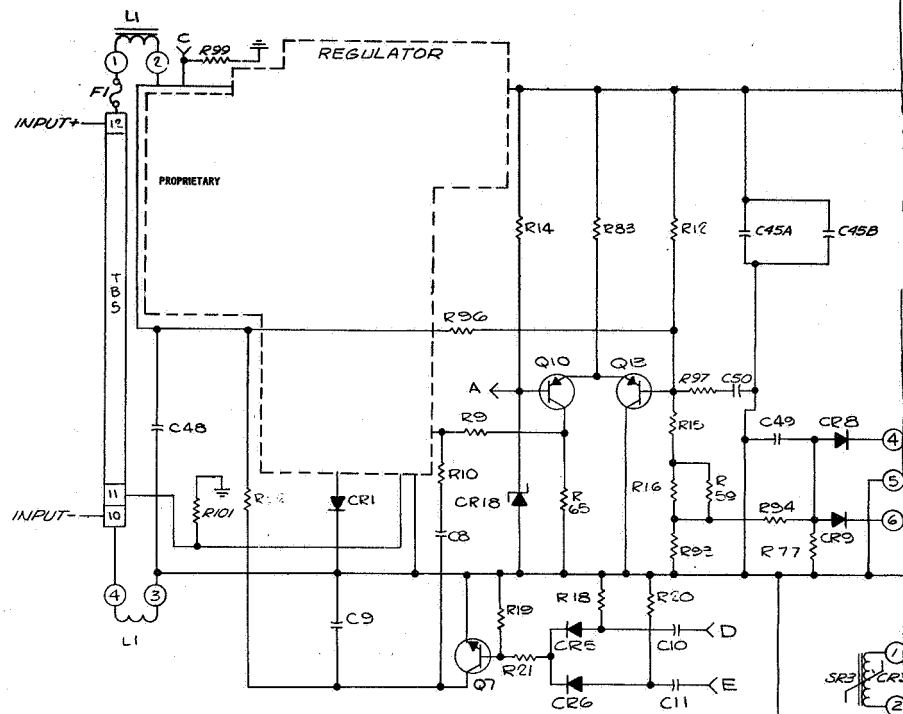


Figure 19



Attenuation of input ripple and transients is achieved by using a high switching frequency (11 kc). This results in fast response, since the half-cycle period is less than 50 microseconds. The tight regulation is achieved by means of a high gain input amplifier used in a closed loop feedback system. The high efficiency is obtained by careful attention to drive waveform and switching patterns in the regulator transistor, and by minimization of the shunt losses. Reliability is obtained by using the minimum number of components to perform the required functions.

As indicated in Figure 20, certain details of the input and regulator are considered to be proprietary by the manufacturer, Engineered Magnetics. It is not therefore possible to present a detailed discussion of its performance. It should be pointed out however that conventional regulator approaches could be taken in the power supply unit with satisfactory performance for application to this tube. The remainder of the supply is discussed in the following paragraphs.

Converter Design Approach

The block diagram shows two converters divided according to voltage. Selection of this arrangement was made after evaluation of various other types of arrangement. It can be seen that at least two converters are needed, since the filament voltage must be applied prior to the application of high voltage. Also, it has been found in the course of test and experimentation that the high voltage converter will be approximately 2% more efficient if it is a driven converter, as contrasted to a self-driven converter. Thus it can be seen that the simplest possible overall arrangement is to have a converter that will generate power for the heater, the drive voltage for the high voltage converter.

Special proprietary techniques are used in the design and manufacture of T2 in order to achieve high efficiency in the high voltage converter as is shown in the block diagram. These special techniques, when used in conjunction with the drive shown for the converter in the schematic,

allow nearly ideal operation of the switching transistors. The operation is ideal in the sense that there are virtually no switching losses because the voltage on the transistor decays before the current rises during turn-on, and the current decays before the voltage rises during turn-off. The special techniques used in winding the transformer are used to reduce the inter-winding capacitance and also to reduce the wire-to-wire capacitance. These parasitic elements are then balanced very carefully against leakage inductance to produce the nearly ideal turn-on and turn-off characteristic.

Filament Converter

The filament converter is a standard magnetically-coupled multivibrator consisting of transistors Q8 and Q9 and transformer T1. The frequency is controlled at 5.5 KHz by the saturable reactor SR1. An investigation has been made and it was determined that frequencies in the range of 5 to 6 kc turn out to be nearly optimum in the sense that they result in the best combination of size, weight, and efficiency. Efficiency is important, not only in meeting the design specification, but high efficiency, in turn, implies reduced component stress level and lowest temperature operation. The filament converter supplies the filament power through saturable reactor SR2. Saturable reactor SR2 is used for voltage adjustment. The saturable reactor is used, since this allows the voltage to be lowered without adding additional losses to the circuit. The filament converter is also used to provide bias for the regulator, sync for the regulator and drive and bias for the high voltage converter.

High Voltage Converter

The high voltage converter is composed of a saturating square wave amplifier consisting mainly of transistors Q19, Q20, and transformer T2. The transformer, T2, has multiple output windings to provide the voltages necessary for the various elements of the tube. These voltages

are consistent with the requirements for 20 watt output from the 219H traveling-wave tube. The high voltages required for the traveling-wave tube anode, collector and helix are derived through full wave bridge rectifiers Z1, thru Z4.

High Voltage Filter

In order to achieve the low output ripple voltages required for the traveling-wave tube assembly, it is necessary to vary carefully design the filters, especially since the high voltage filters occupy the largest volume of any single section to the unit. Three different types of filters are used. For the collector power, a pie-section filter is used, consisting of C28, C27, and L5. For the helix output, an L-section filter, consisting of L3, L4, C26, and C33 is used. For the anode, an L-section filter is used, consisting of R41, C24, R42. An RC filter is used for the anode since the power is so low that a choke would be of prohibitive size. In addition, in order to improve regulation current feedback is used. This consists of T4, CR8, and CR9.

Package Configuration

The power supply and tube was integrated in a traveling-wave tube amplifier package shown in Figure 21. See Appendix C for electrical and mechanical description.

[illegible]

FORM MTD 1036 GAF 12-66 REV.

CONCLUSIONS AND RECOMMENDATIONS

A complete 20 watt, 8.4 to 8.5 GHz traveling-wave tube amplifier consisting of a packaged traveling-wave tube and integral power supply has been developed and delivered to NASA. The traveling-wave tube amplifier was designed for spacecraft applications and meets all of the NASA specification requirements with regard to power, gain and efficiency.

As can be expected in any such state of the art development, numerous areas for future improvement were noted during the development program. These areas of improvement are listed below as recommendations for incorporation into future programs.

Environmental and Life Improvement

The RF "saddle" window used on the present traveling-wave tube design could be replaced with a pipe window design which has been successfully used on more recent tube designs. The pipe window allows traingulation of the helix over its entire length in contrast to the saddle window design where the last turn is under the window and essentially floats thermally. The thermal capability of the helix structure is improved considerably by the change. The pipe window also allows the window ceramic to be further removed by interaction region, which provides better RFI properties since there is no exposed ceramic to allow radiation.

Another area would be to evaluate a change in the method of copper plating the helix from a normal bath-type of plating used for the present tube to vapor deposition.

The latter method has been used on recent tube designs and yields better adhesion and conduction.

Efficiency Improvement

Further work in efficiency improvement could be proposed in the areas of velocity tapering, voltage jump or two-stage collector designs. It is felt that any or all of these methods might be used to provide a significant improvement over the present 35% tube efficiency.

Cost Improvement

A goal, but not a requirement, of the present program was to focus the tube with Alnico magnets which are less expensive and have better thermal properties than the platinum cobalt used. Early experimental tubes were focused with Alnico and results were good, but in an effort to get ultimate efficiency, platinum cobalt was used on the final tube. It is felt that with a slightly scaled gun, tube performance could be as good with Alnico and a savings of approximately One Thousand Dollars per tube might result for future programs. It should be realized that this recommendation may not be completely compatible with efficiency considerations as discussed above, and thereafter should be considered independently.

Weight and Size Improvement

Although the tube and power supply considered individually meet their respective weight and size requirements, the overall package does not represent an optimum design. Again, this arose from the fact that the primary emphasis was placed on the tube development with the power supply being purchased as an off-the-shelf item. Now that the tube parameters are more firmly fixed, an optimum configuration power supply design could be arrived at which would allow the tube and power supply to be packaged into a smaller volume and weight package.

APPENDIX A

219H TWT

ELECTRICAL OPERATING PARAMETERS

| | |
|----------------------|------------------------|
| Beam Voltage | 3400 volts |
| Beam Current | 40 mA |
| Output Power | 20 watts |
| Total Efficiency | 35% |
| Heater Power | 1.2 watts |
| Heater Voltage | 4.5 volts |
| Anode Voltage | 100 volts |
| Collector Depression | 54 - 59% |
| Beam Transmission | 94 - 98% |
| Frequency | 8400 - 8500 Mc |
| Bandwidth | 10 Mc |
| Cathode Loading | 200 mA/cm ² |

APPENDIX B
219H TWT

MECHANICAL PROPERTIES

| | |
|------------------------------|---------------------|
| Length | 10.50 inches |
| Maximum Transverse Dimension | 2.3 inches |
| Height | 1.70 inches |
| Cooling | Conduction |
| Collector to Base ΔT | 9° C |
| Mounting Position | Any |
| Weight | 2.25 lbs. |
| RF Connectors | OSM Female |
| Focusing | PPM Platinum Cobalt |
| Helix ID | .0545 |
| Helix Pitch | .021 |
| Support Rod Diameter | .0385 |
| Support Rod Material | Beryllia |
| Helix Length | 6.30 inches |
| Magnet OD | .650 inch |
| Magnet Period | .270 inch |

APPENDIX C

1153H TWTA

ELECTRICAL AND MECHANICAL DESCRIPTION

| | |
|-----------------------------|---------------------------|
| Length (without connectors) | 11.72 inches |
| Height | 5.0 inches |
| Cooling | Conduction thru baseplate |
| Mounting Position | Any |
| Weight (Total package) | 10 lbs (estimated) |
| RF Connectors | OSM (208) |
| DC power input connector | Bendix PT02A |
| | 14-5P |
| DC Input Voltage | 28 VDC (nominal) |
| RF Power Out (Saturated) | 20 W minimum |

APPENDIX D

DEFINITIONS

| | |
|--------------|---|
| E_k | = Cathode (or beam) voltage (negative with respect of helix ground) |
| I_{tot} | = I_k = cathode current in milliamps |
| E_A | = Anode voltage |
| I_A | = Anode current |
| I_H | = Helix current |
| E_c | = Collector voltage (negative with respect to helix ground) |
| I_c | = Collector current |
| D | = Collector Depression = E_c/E_k (%) |
| T | = Beam transmission = I_c/I_k (%) |
| K | = Efficiency improvement factor = $(1 - TD)^{-1}$ |
| b | = Velocity parameter relating RF phase velocity to beam velocity. |
| μP_B | = Microperveance = $\frac{I_k}{E_k^{3/2}} \times 10^6$ |
| γ | = Radial phase constant |
| r_b | = Beam radius |
| a | = Helix radius |
| QC | = Space charge parameter |
| C | = Gain parameter |
| η_B | = Basic electronic efficiency (collector at helix potential) |
| η_D | = Efficiency with collector depressed (Depressed Efficiency) |
| η_{tot} | = Total (overall) efficiency including filament |
| F | = Frequency |